ISTANBUL TECHNICAL UNIVERSITY ★ GRADUATE SCHOOL

A NUMERICAL INVESTIGATION OF TOTAL TEMPERATURE PROBES MEASUREMENT PERFORMANCE

M.Sc. THESIS

Erdem MERİÇ

Department of Aeronautics and Astronautics Engineering

Aeronautics and Astronautics Engineering Program

JUNE 2023

ISTANBUL TECHNICAL UNIVERSITY ★ GRADUATE SCHOOL

A NUMERICAL INVESTIGATION OF TOTAL TEMPERATURE PROBES MEASUREMENT PERFORMANCE

M.Sc. THESIS

Erdem MERİÇ
(511201122)

Department of Aeronautics and Astronautics Engineering

Aeronautics and Astronautics Engineering Program

Thesis Advisor: Prof. Dr. Fırat Oğuz EDİS

JUNE 2023

ISTANBUL TEKNİK ÜNİVERSİTESİ ★ LİSANSÜSTÜ EĞİTİM ENSTİTÜSÜ

TOPLAM SICAKLIK PROBLARININ ÖLÇÜM PERFORMANSININ SAYISAL BİR İNCELEMESİ

YÜKSEK LİSANS TEZİ

Erdem MERİÇ
(511201122)

Uçak ve Uzay Mühendisliği Anabilim Dalı

Uçak ve Uzay Mühendisliği Programı

Tez Danışmanı: Prof. Dr. Fırat Oğuz EDİS

HAZİRAN 2023

Erdem Meriç, a M.Sc. student of ITU Graduate School student ID 511201122, successfully defended the thesis/dissertation entitled "A NUMERICAL INVESTIGATION OF TOTAL TEMPERATURE PROBES MEASUREMENT PERFORMANCE", which he prepared after fulfilling the requirements specified in the associated legislations, before the jury whose signatures are below.

Thesis Advisor:	**Prof. Dr. Fırat Oğuz EDİS** Istanbul Technical University	.....
Jury Members:	**Prof. Dr. N. L. Okşan Çetiner Yıldırım** Istanbul Technical University	.....
	Dr. Sedat Tokgöz Gebze Technical University	.....

Date of Submission : 31 05 2023
Date of Defense : 23 06 2023

To my family,

FOREWORD

In this M.Sc. thesis, the measurement performance of total temperature probes was investigated using numerical means.

I sincerely thank my advisor, Prof. Dr. Fırat Oğuz EDİS, for his patience, and guidance during this study.

I would like to especially thank my friends Tolga ŞANAP and Can ÖZBARAN for their ideas and continuous support.

Finally, the authors thank KALE R&D management for allowing them to publish the outcomes of this study and the computational resources they provided.

June 2023

Erdem MERİÇ
(Aeronautical Engineer)

TABLE OF CONTENTS

Page

ABBREVIATIONS

AR	**:** Area Ratio
BL	**:** Boundary Layer
CHT	**:** Conjugate Heat Transfer
CT	**:** Conical Tip
DAQ	**:** Data Acquisition
EMF	**:** Electromotive Force
RANS	**:** Reynolds Averaged Navier Stokes
RTD	**:** Resistance Temperature Detector
SST	**:** Shear Stress Transport
ST	**:** Straight Tip
TC	**:** Thermocouple
VKI	**:** Von Karman Institute

SYMBOLS

α_s	: Seebeck Coefficient
T	: Temperature
T_j	: Thermocouple Junction Temperature
T_M	: Thermocouple Wire Mount Region Temperature
T_w	: Duct Wall Temperature
h	: Enthalpy
u	: Internal Energy
P	: Pressure
r	: Recovery Factor
ρ	: Density
V	: Velocity
C_p	: Isobaric Specific Heat
C_d	: Discharge Coefficient
h_c	: Heat Transfer Coefficient
k	: Thermal Conductivity
σ	: Boltzmann Constant
ε	: Emissivity
γ	: Ratio of Specific Heats
Re	: Reynolds Number
Pr	: Prandtl Number

LIST OF TABLES

Page

LIST OF FIGURES

Page

A NUMERICAL INVESTIGATION OF TOTAL TEMPERATURE PROBES MEASUREMENT PERFORMANCE

SUMMARY

In almost every industrial application, the temperature is measured for development and condition monitoring purposes. The accuracy of these measurements is crucial to avoid misunderstandings about the current condition and misguidance in the development phase. The most practical mean of temperature measurement in industrial applications is using a thermocouple. Thermocouples are very flexible structures so they can be applied in many different regions for solid and fluid temperature measurements. It is also possible to design measurement probe geometries using thermocouples as sensing elements.

In machines involving high-speed gas flow, the kinetic energy of fluid can't be neglected in energy interaction calculations so flow must be adiabatically stagnated before temperature measurement. The temperature a flowing fluid gains because of adiabatic stagnation is called stagnation or total temperature.

A stationary probe geometry measures the total temperature of flow but there may be deviations in the temperature of the sensing point due to the flow physics. These deviations lead to errors in measurement. These errors are classified as recovery error, conduction error and radiation error. Recovery error originated from the non-adiabatic stagnation of flow on the surface of the thermocouple (TC) junction. Recovery error is characterized by a parameter called recovery factor which shows the degree of dynamic temperature recovery on the measurement. Conduction and radiation errors arise due to solid boundary conditions which are different from the flow total temperature around the probe. These different temperature zones cause heat interaction via conduction and radiation heat transfer modes between the TC junction and surroundings giving rise to deviations in measurement. Special probe designs are used to prevent these errors.

In this study, an experimental case was selected from the literature to create a conjugate heat transfer (CHT) methodology. This CHT methodology served to investigate flow physics around and inside total temperature probes and the nature of heat interaction between flow and probe geometry. This experimental case contains a total temperature probe calibration setup which investigates the measurement performance of probe geometry under different Mach number flows. In the simulations, the measurement probe geometry was modelled and exposed to the flow at the same speed as the test conditions. The main observed parameter during simulations was TC junction temperature which determines the performance of the total temperature probe. The results of simulations were observed to be in harmony with experimental data. Then, flow structures around and inside the total temperature probe were investigated in detail using the outputs of simulations. The main aim of total temperature probe geometry is to decrease flow velocity inside the shield to decrease thermal conduction in the boundary layer. In simulations, this aim was observed to be accomplished. The flow velocity vectors were investigated to understand the nature of flow around and

inside the total temperature probe. No flow separation was observed on the shield inlet. On the outer surface of the probe shield, a flow separation occurred as expected due to the sharp corner. The flow reattached before reaching the bleed holes and the separation region didn't cause any further limitation on the mass flow rate inside of the shield.

Secondly, a parametric study was carried out to investigate the effect of different probe design parameters and flow conditions on measurement performance. Simulations were done for varying flow angles between 0-30 deg. It was observed that up to 20 degrees flow angle, the measured temperature doesn't deviate from the measured total temperature at the 0-degree flow angle. Probes having a conical shield tip have better performance for greater flow angles, so such geometry is advised if flow angle uncertainty is much. The ratio between the shield inlet area and the total area of bleed holes determines the flow velocity inside the shield and owns a great effect on the recovery factor. As this ratio is increased, the recovery factor is in a trend of increase but after a certain value, its effect is negligible.

In the last part of the parametric study, the effects of flow parameters of temperature and pressure were studied. The effect of temperature was observed to be in correlation with the Prandtl number. An increase in temperature causes a greater recovery factor until reaching the local maximum of the Prandtl number. Then, the relation between temperature and recovery factor becomes inversely proportional. The effect of pressure is more dominant on the recovery factor because the effect of pressure on Reynolds number of flow has a greater order of magnitude than temperature. A higher Reynolds number means a thinner boundary layer and a greater recovery factor so the recovery factor increases with increasing pressure.

Finally, conduction and radiation errors were thermally modelled using basic heat transfer theory. To model these phenomena, the heat transfer coefficient inside the shield had to be formulated in the first place. For the inside of the shield, annular pipe correlation was used, and flow velocity was defined as a function of freestream flow conditions and corrected using the results of CHT simulations. For the outside of the shield, flat plate correlation was applied. To model conduction error, the TC wire was modelled as a one-dimensional fin with a boundary condition defined in the TC wire mount region. TC junction temperatures were investigated for varying TC wire mount temperatures. It was observed that TC junction temperature may deviate considerably so area ratio must be carefully controlled to avoid conduction error.

To model radiation error, the TC wire is modelled as a body enclosed by the shield. The shield is also enclosed by a duct wall whose temperature is different from the flow total temperature. Application of shield is observed to be a very effective precaution as the errors are less than %1,5 even in the very low-speed application of AR-4 but for a total temperature of 1000 K measured temperature deviated more than 10 K for AR-4 case so AR must be controlled carefully considering flow speeds at the measurement location to avoid radiation error.

To sum up, the fundamentals of temperature measurement in high-speed and temperature environments were explained. A CHT methodology was constructed to investigate flow structures inside and around of total temperature probe geometry. The effects of probe design parameters and flow conditions were studied. Lastly, thermal models were generated to investigate the conduction and radiation error mechanisms.

TOPLAM SICAKLIK PROBLARININ ÖLÇÜM PERFORMANSININ SAYISAL BİR İNCELEMESİ

ÖZET

Hemen hemen her endüstriyel uygulamada, katı ve akışkan sıcaklıkları, geliştirme ve durum izleme amaçları için ölçülür. Bu ölçümlerin doğruluğu, mevcut durumla ilgili yanlış anlamaları ve geliştirme aşamasındaki olası yanlış yönlendirmeleri önlemek adına önem arz etmektedir. Endüstriyel uygulamalarda sıcaklık ölçümünün en pratik yolu, pasif bir eleman olan ve ölçülen sıcaklıkla bağıntılı bir gerilim değeri üreten termokuplları kullanmaktır. Termokupllar oldukça esnek yapılardır. Bu nedenle katı ve akışkan sıcaklık ölçümleri için pek çok farklı bölgede uygulanabilirler. Algılama elemanları olarak termokupllar kullanılarak ölçüm probu geometrileri tasarlamak da mümkündür.

Yüksek hızlı gaz akışı içeren makinelerde, enerji etkileşimi hesaplamalarında akışkanın kinetik enerjisi ihmal edilemez. Bu nedenle sıcaklık ölçümünden önce akışın adyabatik olarak durağanlaştırılması gerekir. Hareket halindeki bir akışkanın adyabatik durağanlaşma sonucu kazandığı sıcaklığa durgunluk sıcaklığı veya toplam sıcaklık denir. Sabit bir ölçüm probu ile yalnızca, bir gaz akışının toplam sıcaklığı ölçülebilir, çünkü prob tasarımından bağımsız olarak akış her zaman ölçüm noktası üzerinde bir dereceye kadar durağanlaşacaktır. Bir ölçüm probunun statik sıcaklığı ölçebilmesi için akışla aynı hızda hareket etmesi gerekmektedir.

Sabit bir prob, akışın toplam sıcaklığını ölçmektedir ancak akış fiziğinden dolayı prob içerisindeki algılama elemanının eriştiği sıcaklığın, akışın toplam sıcaklığından sapma ihtimali vardır. Bu sapma ölçüm hatasına yol açmaktadır. Bu hatalar, geri kazanım hatası, iletim hatası ve radyasyon hatası olarak sınıflandırılmaktadır. Geri kazanım hatası, termokupl (TC) bağlantı noktasının yüzeyinde akışın adyabatik olmayan halde durağanlaşmasından kaynaklanmaktadır. TC bağlantı noktası, bir termokuplun ölçüm noktasıdır ve termokupl TC bağlantı noktasının ulaştığı sıcaklığı ölçüm değeri olarak çıktı vermektedir. Geri kazanım hatası, ölçümde dinamik sıcaklık geri kazanımının derecesini gösteren ve geri kazanım faktörü adı verilen bir parametre ile karakterize edilmektedir. İletim ve radyasyon hataları, prob çevresinde akış toplam sıcaklığından farklı sıcaklık değerlerine sahip katı bölgeler olması halinde ortaya çıkmaktadır. Bu farklı sıcaklık bölgeleri TC bağlantı noktası ile, iletim ve radyasyon ısı transferi mekanizmaları yoluyla enerji etkileşimi gerçekleştirir. Bu ısı akışı sonucu ölçümde hatalar meydana gelebilir. Bu hataların önüne geçmek için özel prob tasarımları kullanılmaktadır. Literatürde önerilmiş olan prob tasarımları, değişken akış koşulları altında deneysel olarak kalibre edilmiştir. Bu kalibrasyon çalışmalarında probların farklı akış koşulları altında geri kazanım faktörü değerleri belirlenmiştir. İletim ve radyasyon hatalarını önlemek adına, prob geometrileri bu amaca hizmet edecek halde

tasarlanmıştır. Bu hata kaynaklarının etkilerini belirleyebilmek adına ise korelasyonlar önerilmiştir.

Bu çalışmada, toplam sıcaklık problarının etrafındaki ve içindeki akış fiziğini ve akış ile prob geometrisi arasındaki ısı etkileşiminin doğasını araştırmak üzere bir eşlenik ısı transferi (CHT) metodolojisi oluşturulmuştur. Oluşturulan CHT metodolojisini valide etmek için literatürden deneysel bir çalışma belirlenmiştir. Bu deneysel çalışma, farklı Mach sayılarında hızlara sahip akışa maruz bırakılmış prob geometrilerinin ölçüm performansını araştıran bir toplam sıcaklık probu kalibrasyon test düzeneğini içermektedir. Simülasyonlarda ölçüm prob geometrisi modellenmiş ve test koşulları ile aynı hızda akışa maruz bırakılmıştır. Simülasyonlar sırasında gözlemlenen ana parametre, toplam sıcaklık probunun performansını belirleyen TC bağlantı noktası sıcaklığıdır. Simülasyon sonuçlarının deneysel verilerle uyum içinde olduğu gözlemlenmiştir. Daha sonra simülasyon çıktıları kullanılarak toplam sıcaklık probunun etrafındaki ve içindeki akış yapıları detaylı olarak incelenmiştir.

Toplam sıcaklık probu geometrisinin ana amacı, sınır tabaka içerisindeki termal iletimi azaltmak adına prob kalkanının içindeki akış hızını düşürmektir. Simülasyonlarda bu amaca ulaşıldığı görülmüştür. Simülasyon sonuçları üzerinden adyabatik olmayan durağanlaşmanın sebebi araştırılmıştır. TC bağlantı noktasının etrafında oluşan sınır tabakada, statik sıcaklıktaki gradyanlara yol açan hız gradyanları meydana gelmektedir. Statik sıcaklık gradyanı nedeniyle akışkan enerjisinin bir kısmı TC bağlantı noktası yüzeyinden serbest akışa iletilir. Böylece; sınır tabakanın TC bağlantı noktası üzerinde konumlanan ilk katmanında, akış hızı sıfır olmasına rağmen serbest akış toplam sıcaklığına ulaşılamaz. Bu durum, viskoz etkilerin ve termal iletkenliğin bir sonucudur. Toplam sıcaklık probunun etrafındaki ve içindeki akışın doğasını anlamak için akış hızı vektörleri incelenmiştir. Kalkan giriş bölgesinde akım ayrılması gözlemlenmemiştir. Prob kalkanının dış yüzeyinde bulunan keskin köşe nedeniyle, beklendiği gibi bir akım ayrılması meydana gelmiştir. Bu akım ayrılmasının sızdırma deliklerine ulaşmadan önce tekrar kalkan yüzeyiyle birleştiği ve ayrılma bölgesinin, kalkanın içinden geçen kütlesel hava debisi üzerinde bir sınırlamaya neden olmadığı gözlemlenmiştir.

İkincil olarak, farklı prob tasarım parametrelerinin ve akış koşullarının ölçüm performansı üzerindeki etkisini araştırmak için bir parametrik çalışma gerçekleştirilmiştir. 0-30 derece arasında değişen akış açıları için simülasyonlar yapılmıştır. 20 dereceye kadar ölçülen sıcaklığın 0 derece koşulundaki ölçümden sapmadığı görülmüştür. Konik bir kalkan ucuna sahip olan probların daha büyük akış açıları için daha iyi performansa sahip olduğu gözlemlenmiştir. Bu nedenle akış açısı belirsizliğinin yüksek olduğu durumlarda bu tip bir geometri önerilmektedir. Kalkan giriş alanı ile boşaltma deliklerinin toplam alanı arasındaki oran, kalkan içindeki akış hızını belirler ve geri kazanım faktörü üzerinde büyük bir etkiye sahiptir. Bu oran arttıkça geri kazanım faktörü artma eğiliminde olmakla birlikte, bir değerden sonra etkisi ihmal edilebilir düzeydedir. Geri kazanım faktörünü artırmak için akış hızının düşürülmesi her durumda faydalı olmayabilir çünkü daha düşük hız, daha düşük ısı transfer katsayısı (HTC) anlamına gelir. Eğer probun bulunduğu ortamda iletim ve radyasyon hatalarına sebep olacak farklı katı sıcaklık bölgeleri mevcutsa bu hata kaynakları, akışın ısı transfer katsayısının düşük olması durumunda daha baskın hale gelir. Bu nedenle, ölçüm yapılan koşullar dikkate alınarak alan oranı dikkatle kontrol edilmelidir.

Parametrik çalışmanın son bölümünde ise akış parametreleri olan sıcaklık ve basıncın etkileri incelenmiştir. Sıcaklığın etkisinin Prandtl sayısı ile korele olduğu gözlemlenmiştir. Prandtl sayısı arttıkça akış termal olarak daha az difüzif hale geldiği için duvardaki ilk katmanın sıcaklığı akış toplam sıcaklığına yaklaşmaktadır. Belirli bir sıcaklık değerinde Prandtl sayısı yerel bir maksimuma ulaşır ve azalmaya başlar. Bu nedenle, geri kazanım faktörü üzerindeki sıcaklık etkisi doğrusal değildir. Sıcaklıktaki artış, Prandtl sayısı yerel maksimum değerine ulaşana kadar geri kazanım faktöründe artışa neden olur. Prandtl sayısının yerel maksimum değerinden sonraysa, sıcaklık ile geri kazanım faktörü arasındaki ilişki ters orantılı hale gelir. Basıncın etkisi geri kazanım faktörü üzerinde daha baskındır, çünkü basıncın akış Reynolds sayısı üzerindeki etkisi sıcaklıktan daha büyük bir mertebeye sahiptir. Daha yüksek Reynolds sayısı, daha ince bir sınır tabaka ve daha büyük geri kazanım faktörüne sebep vermektedir. Bu nedenle akışkan basıncındaki artışın, geri kazanım faktörünü yükselttiği gözlemlenmiştir.

Son olarak; iletim ve radyasyon hataları, temel ısı transferi teorisi kullanılarak termal olarak modellenmiştir. Bu fenomenleri modellemek için, ilk etapta prob kalkanı içerisindeki akışın ısı transfer katsayısının formüle edilmesi gerekmektedir. Kalkanın içi için halkasal boru korelasyonu kullanılmıştır. Akış hızı serbest akış koşullarının bir fonksiyonu olarak tanımlanmış ve CHT simülasyonlarının sonuçları kullanılarak düzeltilmiştir. Kalkanın dışı içinse düz plaka korelasyonu uygulanmıştır. İletim hatasını modellemek için, TC teli tek boyutlu bir fin olarak modellenmiştir. TC telinin proba bağlandığı noktada bir katı sıcaklık sınır koşulu tanımlanmıştır. TC bağlantı noktası sıcaklıkları, TC telinin proba bağlandığı noktanın değişken sıcaklıkları için incelenmiştir. TC bağlantı sıcaklığının önemli ölçüde değişebileceği gözlemlenmiştir. Bu nedenle iletim hatasını önlemek için alan oranının dikkatli bir şekilde kontrol edilmesi gerekmektedir.

Radyasyon hatasını modellemek için TC teli, kalkanla çevrelenmiş bir gövde olarak modellenmiştir. Kalkan sıcaklığı akış toplam sıcaklığından farklı bir değere sahip olan duvar tarafından çevrelenmektedir. Alan oranının 4 olduğu çok düşük bir hız durumunda bile hatanın %1,5'ten daha az olduğu gözlemlendiği için kalkan uygulamasının etkili bir önlem olduğu sonucuna varılmıştır. Ancak 1000 K toplam sıcaklık değeri için alan oranının 4 olduğu koşul altında ölçülen sıcaklık 10 K'den fazla saptığı için yüksek sıcaklıklarda radyasyon hatasının dikkate alınması gerektiği gözlemlenmiştir. Radyasyon hatasını önlemek için akış hızları göz önüne alınarak alan oranı dikkatli bir şekilde kontrol edilmelidir.

Özetle, bu çalışma kapsamında yüksek hız ve sıcaklık ortamlarında sıcaklık ölçümünün temelleri anlatılmıştır. Toplam sıcaklık probu geometrisinin içindeki ve çevresindeki akış yapılarını araştırmak için bir CHT metodolojisi oluşturulmuştur. Prob tasarım parametrelerinin ve akış koşullarının ölçüm performansı üzerindeki etkileri incelenmiştir. Son olarak, iletim ve radyasyon hata mekanizmalarını araştırmak için termal modeller üretilmiştir.

1. INTRODUCTION

Measuring temperature accurately is a very important requirement during the development phase and service life of many industrial products. In aerospace vehicles, structural materials are required to work under harsh environments with excessive temperature values. Because of that, it is very important to accurately measure material temperatures to examine the capability of a structure to stand the loads during operation and to optimise the design for weight reduction. It is also essential for an aerospace vehicle to consume a low amount of fuel to decrease the weight of the structure and cost of operation. A machine generating thrust or power shall be thermodynamically efficient to be able to consume a low amount of fuel. To have a thermodynamically efficient machine, it must be aerodynamically well-designed with low entropy production during its cycle. This aerodynamic design should be carefully investigated with heavy instrumentation. One of the most important measurement parameters is the total temperature of flowing gas because changes in total temperature directly tell how much work a component has done to gas or extracted from high-energy gas.

The measurement of temperature is usually done on two different media in industrial applications. The first one is the measurement of metal temperatures. This is achieved using thermocouples directly connected to the measurement surface. Error sources are minimal in such an application. Thermocouple junction should be properly connected to the measurement point via welding or a similar method and there must be no thermal resistance generating element between the junction and measurement point. Secondly, the temperature of flowing gas is measured to make performance calculations. On the flow field, flow velocity may even reach supersonic speeds in some areas. Due to such high speeds, the kinetic energy of flow can't be neglected. Thus, the total temperature of the flow must be measured accurately to be able to assess the energy content of the flow.

Specific probe geometries are used to be able to measure the total temperature of flow accurately. When measuring temperature with a thermocouple or a similar instrument,

the indicated temperature of the measurement device is essentially the solid temperature of a specific point which reaches thermal equilibrium under different boundary conditions. In total temperature measurement, there are errors arising from different heat transfer mechanisms of conduction, convection, and radiation. Probe geometries are designed in a way which tries to minimize the effects of these error sources and quantify them for different operating conditions. This study will concentrate on discussing the roots of these error mechanisms using the results of validated numerical simulations and proposing design practices to minimize measurement error. In addition, calculation methodologies to quantify possible errors will be proposed.

1.1 The Concept of Temperature and Its Measurement

Temperature is the measure of hotness and coldness practically and it determines the direction of heat flow from hotter material to colder one.

To understand temperature with deeper insight, the concept of internal energy shall be investigated in the first place. Molecular activity in the structure of matter involves the translational motion of molecules, the rotational and vibrational motion of atoms in polyatomic molecules and electrons rotating around the nucleus in each atom. All these individual motions are sources of kinetic energy. The total of all molecular kinetic energy is defined as sensible energy. The average kinetic energy of molecules is proportional to temperature. Thus, temperature is a representation of the sensible energy of a matter [1].

The internal energy of matter comprises three more components: latent energy (the potential energy due to the binding forces between molecules), chemical energy (the potential energy associated with atomic bonds), and nuclear energy (the potential energy associated with bonds between particles in the nucleus). These three energy components don’t have a direct relation with temperature and don’t change unless a phase change, a chemical reaction or a nuclear reaction occurs [1].

To describe temperature numerically, temperature scales are defined. Phase change points under specific pressure have a constant temperature. Thus, they are used as references for temperature scales. Celsius and Fahrenheit scales are used in the Metric and English systems respectively. They take the freezing point of water under 1 atm

pressure as 0 Celsius and 32 Fahrenheit, and the boiling point of water under 1 atm pressure as 100 Celsius and 212 Fahrenheit. For scientific studies, a temperature scale which is independent of any material had to be produced. The Kelvin Scale determines 0 Kelvin as absolute zero which means the minimum reachable temperature in the universe. Theoretically, at 0 Kelvin whole molecular motion stops [1].

All measurements rely on a very simple fundamental idea. The physical property which is desired to be measured shall be an input parameter to a specific property of the material of the measuring device. When this physical parameter changes, the observed property of the material also changes with a repeating pattern. This pattern can be expressed as a physical formula.

For daily uses, the temperature is measured with thermometers exploiting the thermal expansion of liquid mercury depending on temperature change. For scientific and industrial applications, thermocouples are widely used due to their simplicity and cheapness. There are other methods of measuring temperature such as Resistance Temperature Detectors (RTD) which uses the change of an electrical resistance under varying temperature, Infrared Temperature Sensors which transforms the intensity of emitted thermal radiation from a body into its temperature and special chemicals which changes their colour under specific temperature values. As this thesis concentrates on temperature probes using thermocouples as measuring devices, only thermocouples will be widely explained.

1.2 Thermocouples

Thermocouples depend on a physical principle called Seebeck Effect. If each end of an electrical conductor wire is at different temperatures, a voltage difference also occurs between these points generating an electromotive force (emf). The magnitude of this electromotive force depends on the temperature difference and type of wire material.

$$\varepsilon = \int_{T_1}^{T_2} \alpha_s(T)dT \tag{1.1}$$

Where ε is electromotive force (emf), α_s is Seebeck Coefficient, which is temperature dependent and unique for each material, T_1, T_2 are reference and measurement point temperatures of wire respectively.

As seen in equation 1.1, generated emf doesn't depend on temperature distribution on wire or wire dimensions. Emf generated along a single wire can't be measured because if an additional wire is used to connect a voltmeter to both ends of the wire then this wire will also generate an emf due to the temperature gradient it is exposed to. Thus, the measured value on the voltmeter will also include the effects of the other wire [2].

A thermocouple is made of two different wires to overcome this problem. In this configuration emf measuring wires are in the reference region. Thus, no temperature gradient exists along these wires. The voltmeter shows the difference between emf generated by different materials under the same temperature difference. Thermocouples must be calibrated to define the relationship between temperature difference and measured voltage. Figure 1.1 shows a typical thermocouple structure in which two wires made of different materials are connected at the junction end whose temperature is desired to be measured. At the reference temperature region, a known temperature value is set. Voltmeter and its connecting wires which are positioned in a region where no temperature gradient exists measure the electrical potential difference between each thermocouple wire.

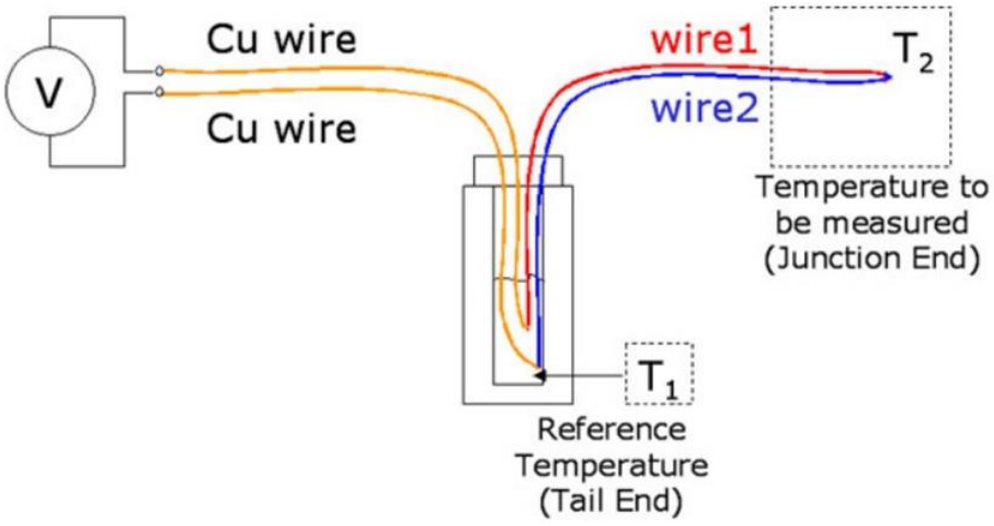

Figure 1.1: A Typical Thermocouple Structure [2].

Generated emf is a function of temperature difference but our main aim is to measure the exact value of temperature. Therefore, we need to know the temperature value at the other end of the wires which is called reference temperature. An ice bath where water exists in solid and liquid phases guarantees a 0 C temperature at 1 atm pressure is used to create a reference temperature. In industrial applications, an electronic circuit called cold junction compensation is used. Data Acquisition (DAQ) equipment on the market employs different electronic circuits to carry out this task. In one example, a temperature-sensitive resistance element is thermally integrated into a reference junction, a reference temperature is set usually as 0 C. If the ambient temperature deviates from the set value, a thermally generated voltage appears and compensates for the change in reference temperature [2].

Thermocouple wires are usually isolated inside a ceramic powder to avoid the chemical interaction of wires with the surrounding atmosphere and electrical noise. Magnesium oxide (MgO) is generally used for this aim. Also, a metallic piping called as sheath retains this structure to increase mechanical strength. A sectional view of a typical thermocouple is illustrated in Figure 1.2.

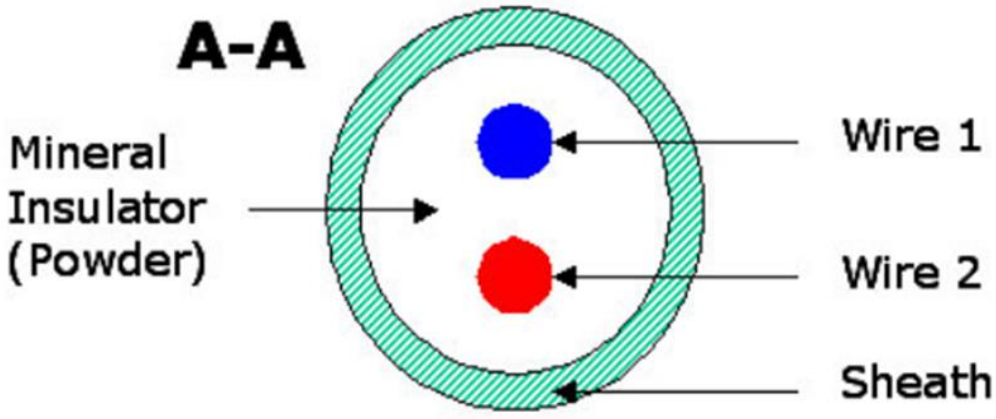

Figure 1.2: A Sectional View of a Typical Thermocouple [2].

1.3 The Concept of Total Temperature and Total Temperature Measurement Probes

Enthalpy is a widely used concept in flow processes and is defined as the sum of internal and flow energy.

$$h = u + \frac{P}{\rho} \tag{1.2}$$

Where h is the enthalpy of fluid, u is the internal energy of fluid, P and ρ are fluid pressure and density respectively. If the flow is low speed and potential energy is negligible, the enthalpy of flow can be considered as the total energy of the flowing fluid. In gas flows, the velocity of flow may increase to ranges where the kinetic energy of bulk motion also comes into play. To show the total energy of a flowing fluid in such cases, a new concept called total enthalpy is defined.

$$h_t = h + \frac{V^2}{2} \tag{1.3}$$

Where, h_t is the total enthalpy of flow and V is flow velocity. Total enthalpy also called stagnation enthalpy is the sum of internal energy, flow energy and kinetic energy of a flowing fluid. The total enthalpy of flow in a control volume doesn't change unless heat transfer or work interaction occurs along the boundaries of a control volume. If the flow is stagnated adiabatically all kinetic energy of the flow is transformed into enthalpy.

Stagnation properties define the properties of a flowing fluid at rest. Total temperature is defined as the temperature of a flowing fluid when it stagnates adiabatically. Total temperature is an imaginary concept to show the energy content of a fluid stream. Under the assumption of an ideal gas.

$$T_t = T + \frac{V^2}{2C_p(T)} \tag{1.4}$$

Where T_t is the total temperature of flowing fluid and $C_p(T)$ is the isobaric-specific heat of fluid which is a function of the temperature of fluid.

1.4 Total Temperature Measurement Probes

When a sensor is placed inside a flow field. It is stationary. Thus, the flow stagnates on the sensor. As it was explained in Section 1.3, the total temperature is the temperature the fluid gains under adiabatic stagnation. To be able to measure total temperature correctly, a probe geometry must be designed to provide adiabatic stagnation of flow on the surface of the sensing element.

Total temperature probes generally use thermocouples as sensing elements because their flexible structure is suitable enough to create various probe geometries. The output of the temperature probe should be routed to a reference junction with the same type of thermocouple wires not to change Seebeck coefficients along the measurement chain. Thermocouples after being placed inside a probe must be calibrated in static conditions. At the same time, the components of the data acquisition system (filter, amplifier, analogue to digital converter) must also be properly calibrated to increase measurement accuracy [3].

Besides the thermocouple and DAQ performance, the effectiveness of a total temperature probe geometry is crucial for measurement accuracy. The probe design is shaped by the requirements and availabilities of the process. Total temperature probes are divided into two main categories. The first type is bare-wire ones in which the junction of thermocouple wire directly sees the flow and is not enclosed by a shield. This configuration has a lower response time and is easier to construct. In high-velocity and temperature environments, the thermocouple junction is retained by a shield geometry which reduces the flow velocity the thermocouple junction sees and minimizes errors due to thermal radiation.

While measuring total temperature, some error sources exist due to flow physics. These errors are recovery error, conduction error and radiation error.

1.4.1 Recovery Error

When a fluid stream flows over a body, flow is slowed due to the no-slip condition on the surface of the body. During this process, the kinetic energy of the flow is converted into internal energy, resulting in a local rise in the static temperature of the flow. The flow velocity isn’t uniform along the boundary layer (BL) (on the surface of the body all kinetic energy is lost whereas, areas far away from the solid surface preserve a

portion of its kinetic energy). Thus, temperature non-uniformities in the BL occur leading to thermal conduction of heat energy from hotter areas to colder ones. This phenomenon is the source of recovery error resulting in lower temperature values on fluid-solid interface than freestream total temperature [4].

If a thermocouple junction is taken into consideration, it is also a body immersed in a fluid stream. Thus, on the interface between the junction surface and fluid, temperature always becomes less than the flow total temperature. This phenomenon leads to temperature readings less than the flow total temperature although the thermocouple is statically calibrated and the DAQ system works with a good performance. This error is purely aerodynamic and the only way to decrease this error is to study the geometry of the total temperature measurement probe.

The recovery factor is defined as,

$$r = \frac{T_j - T_s}{T_t - T_s} \tag{1.5}$$

Where T_j is indicated temperature reading on the thermocouple junction, T_t and T_s are flow freestream total temperature and static temperature.

As seen from equation 1.5, the recovery factor is a measure of the 'recovery' of dynamic temperature on the surface of a solid body. It can't take a value greater than 1. Well-designed probes own recovery factor values of more than 0.9 for varying flow conditions. The recovery factor is mostly a function of flow Mach number, Reynolds number also affects boundary layer structure but is generally neglected under high-pressure values which is usual for high-speed machine flow field.

To increase dynamic temperature recovery on thermocouple junction, probe designs as shown in Figure 1.3 are used. In such a design, the flow enters through the thermocouple shield and exits from the holes downstream of the thermocouple junction. Bleed holes set the mass flow rate of gas entering the shield if the bleed holes own a smaller sectional area, they restrict the mass flow rate passing through the shield inlet and decrease the velocity of gas entering the shield.

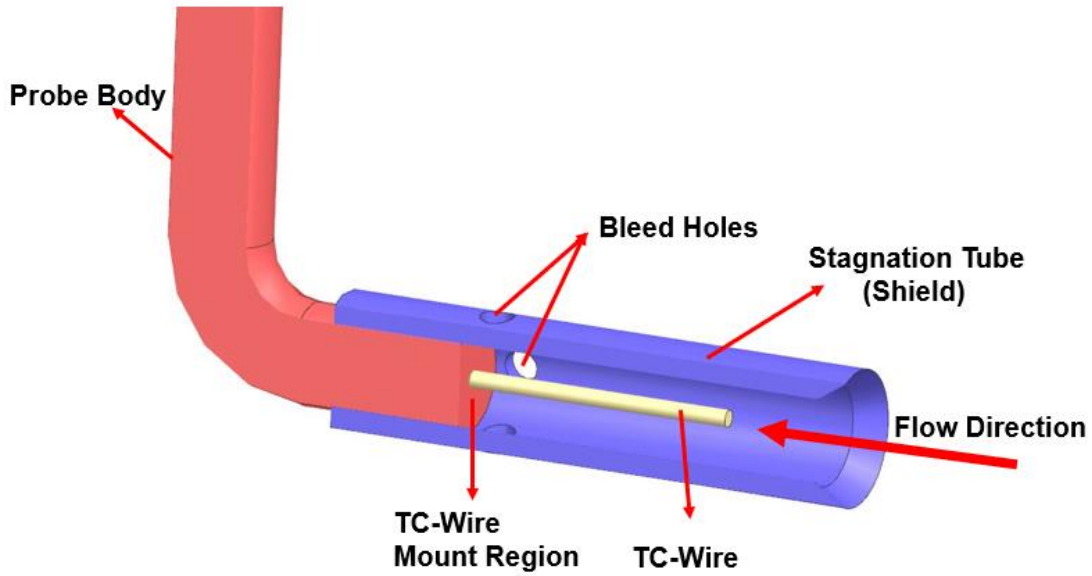

Figure 1.3: A Typical High Recovery Total Temperature Probe.

The recovery factor is generally characterized by a specific probe design with free jet tests. In these tests, an atmospheric jet is conditioned to supply specific Mach number values on the measurement probe, a test rig like the one in Figure 1.4 is used in such applications. A plenum chamber where the flow is assumed to be stagnant is pressurized to match the desired Mach number at the nozzle outlet. No temperature conditioning is applied because only the effect of Mach number is investigated in such a study.

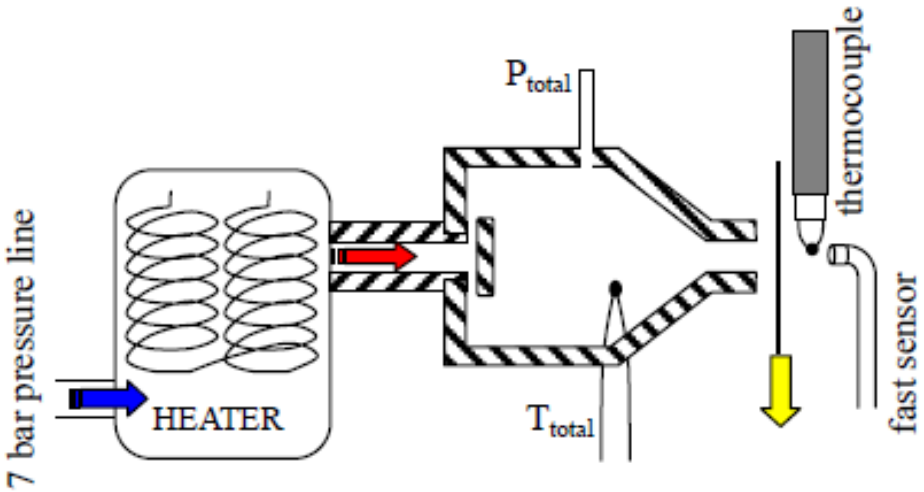

Figure 1.4: VKI Probe Calibration Setup [4].

1.4.2 Conduction Error

As seen in Figure 1.3, the air stream flows around the TC wire and junction after entering the shield and the thermocouple wire is mounted to the probe support. If probe support is mounted to a region whose temperature is different from the flow total temperature, it may affect the solid temperature TC junction leading to heat flow from the TC junction to the wire mount resulting in a deviation between TC junction temperature and flow total temperature. TC wire can be modelled as a one-dimensional fin where air flows on a protruding bar. Using the heat transfer theory of fins assuming an adiabatic tip, the following equation is derived [3].

$$T_t - T_j = \frac{T_t - T_M}{cosh\left[L\left(\frac{4h_c}{Dk_s}\right)^{\frac{1}{2}}\right]} \tag{1.6}$$

Where T_t, T_j are flow total temperature and junction temperature respectively. T_M is the solid temperature where the thermocouple wire is mounted to the probe strut, L is the length of the thermocouple wire, h_c is the heat transfer coefficient inside the shield.

Considering equation 1.6, to decrease the conduction error;

$T_t - T_M$ may be reduced. This difference occurs due to the heat conduction from the probe mount to a region where the probe is connected. The heat also interacts between the probe strut and the airflow around it. With a certain type of insulation, heat conduction to duct wall can be minimized but the heat interaction between flow and probe strut is very hard to control.

L/D can be increased. This is the most practical method to decrease conduction error. An increase in this ratio increases the dominance of convective heat transfer to the conductive heat transfer on the TC wire leading to a smaller temperature gradient through the TC wire. Similar applications propose a value of 15 is mechanically achievable but the designer should evaluate the conditions the probe will work to preserve the probe [3].

h_c can be increased.

$$h_c = \frac{Nu\, k_f}{D} \tag{1.7}$$

Where, h_c is the heat transfer coefficient inside the shield, Nu is the Nusselt number of flow inside the shield, k_f is gas thermal conductivity and D is thermocouple wire diameter. Flow velocity inside of shield must be increased to increase h_c. As discussed in Section 1.4.1, this increases recovery error. The designer should make a choice evaluating the relative importance of conduction and recovery errors.

An alternative solution is heating the thermocouple base to set the T_M same as the T_j using an electric coil. Although the results of this study are satisfactory, it is very impractical to apply in the field and not accepted as a rule [5], [6].

1.4.3 Radiation Error

If there is a considerable temperature difference between the thermocouple junction and surroundings, thermal energy is radiated outwards or inwards thermocouple junction. Generally, a thermocouple junction is hotter than the surroundings because the thermocouple is usually positioned in a duct where hot flow occurs and the walls cool down due to interaction with ambient temperature or some sort of cooling mechanism. Shield of the probe again plays a critical role to decrease this error type blocking the direct view between the junction and surroundings.

Neglecting other heat transfer mechanisms other than convection along the thermocouple wire and radiation of thermocouple junction to the surrounding environment, radiation error can be expressed as;

$$T_t - T_j = \frac{\sigma \varepsilon}{h_c}\left({T_j}^4 - {T_w}^4\right) \tag{1.8}$$

Where T_w is surround wall surface temperature, σ is Boltzmann constant, ε is the emissivity of the thermocouple junction.

To decrease radiation error a multi-shield approach may be implemented. Reference no.7 studied a five-shield-containing probe and derived the following equation to show the effect of shield number on radiation error [7].

$$Y_{R,S} = \frac{1}{n+1} Y_{R,B} \tag{1.9}$$

Where, $Y_{R,S}$ radiation error with the shield, $Y_{R,B}$ is bare-wire radiation error, and n is number shields. The position of the thermocouple junction also can be optimized to

create a minimum view factor with surroundings. Coating thermocouple junctions with a low-emissivity material is a method some researchers tried either [4].

1.5 Literature Review

When the time reached the second half of the 1940s, high-speed air vehicles were starting to fly in the skies. This phenomenon was also the beginning of the competition between different countries. The desire for making faster and more efficient flying machines brought the necessity of long test campaigns in which lots of data would be gathered with the greatest accuracy possible. To satisfy this requirement, many researchers have studied to create accurate methods for total temperature measurement. Their efforts were experimental, and their main goal was to standardize a bunch of probe geometry for specific applications and create correlations to correct possible measurement errors.

Reference no. 8 made a study on total temperature probe performance in a supersonic environment. Short and blunt type shields were preferred to long and thin ones because such a type causes a detached bow shock upstream of the shield. Thus, the air sample enters the shield at subsonic speed giving rise to thicker thermal boundary layers around the shield and the possibility of flow separation due to shock boundary layer interaction or adverse pressure gradients inside of the shield is lower. [8].

In Reference no. 9, an experimental campaign was conducted to determine time constants and Nusselt numbers of bare-wire thermocouple probes under high velocity and temperature conditions. They derived Nusselt number correlations for different probe configurations and methods to calculate conduction and radiation errors. But the correction methodologies are too complex for the data reduction process [9].

Reference no. 10 concentrated on determining recovery and time constant characteristics for different probe designs in subsonic and supersonic regimes. Three shielded and three unshielded probes were tested. Bare wire ones have lower time constants as expected. In the shielded ones, the effect of Mach number and flow angle on the recovery factor was observed to be negligible. An important observation of this study is that for supersonic cases thermocouple junctions should be positioned downstream of shock waves to avoid large recovery errors [10].

Reference no. 11 carried out a study to investigate response characteristics of thermocouples for jet engine control. They made an experimental study on a test rig which can supply continuous flow up to 1300 K. It was observed that time response is a strong function of mass flow rate inside of shield because the convective heat transfer is dominant in rapid heating and cooling periods [11].

Reference no. 12 made an experimental determination of recovery and radiation characteristics for several bare-wire and shielded temperature probe designs to standardize some probe geometries to avoid calibration costs [12].

These experimental efforts created a guideline for temperature measurement in high-speed and high-temperature flows. Some studies were also conducted to solve specific problems both experimentally and analytically. Reference no.13 using all existing experimental backgrounds derived some correlations for Nusselt numbers on thermocouples in different configurations [13]. Reference no.3 prepared an extensive document to point out critical points in gas path measurements of a jet engine. In this document, instrumentation determination and positioning, aerodynamic probe designs and necessary data acquisition systems were discussed [3]. Reference no.5 conducted a study to evaluate the performance of thermocouple probes to be used at short-duration facilities where unsteady measurement errors are also not negligible. The probe designs were tested in a hot jet apparatus to evaluate the steady and dynamic responses of sensors. Recovery factors of different probes for a varying Mach number range were acquired experimentally [5].

After the emergence of fluid flow simulation methods and their widespread usage in industry and academia paved the way for a more detailed investigation of flow characteristics in and around the probes. Reference no.14 conducted CHT simulations for a rake-type shielded temperature probe under varying Reynolds and Mach numbers to investigate flow structures and parametric dependencies of error sources [14]. Reference no.15 has written a graduate thesis about total temperature probe computational modelling. In this study, the CHT approach was validated with experimental data and flow structures were investigated. A new probe geometry aiming to reduce conduction error was also discussed [15]. Reference no.4 studied the thermal performance of total temperature probes using CHT and correlated heat transfer coefficients as a function of Reynolds and Stanton numbers which depend on the geometric characteristics of the probe [4]. Reference no.16 conducted a

comprehensive study using CHT. In their study, they modelled a temperature probe mounted in an exhaust duct. All heat transfer modes are active in their simulations. Although the CHT methodology and comparisons with analytical calculation seem consistent, CHT results weren't experimentally validated and the models are applicable for simple flow cases unlike the one in a jet engine [16].

1.6 Purpose of Study

In this study, the importance of accurate temperature measurement on industrial products was stated. Secondly, possible error sources while measuring the total temperature of flow in a high velocity and temperature environment were described. A conjugate heat transfer (CHT) methodology will be constructed to analyse flow structures inside and around the total temperature probe flow field. To validate constructed CHT methodology, the results of an experimental campaign which was made to characterize certain probe designs in terms of possible measurement errors will be compared with the results of CHT simulations. CHT simulations will be carried out in a domain where no radiation or conduction error exists. Thus, deviations in probe measurement are purely recovery errors. After an investigation of simulation results, the effects of different probe design parameters and flow conditions on measurement accuracy will be discussed. Finally, calculation methodologies will be constructed to evaluate the effects of different error mechanisms using the outputs of simulations. The main aim of this study is to create a guideline for any experimentalist to design optimum total temperature probes for high velocity, high temperature and harsh environments.

2. VALIDATION STUDY

A Conjugate Heat Transfer (CHT) analysis methodology will be constructed in the context of this study. To validate the CHT methodology, experimental data from [12] will be used. Lewis Research Center conducted a study to standardize thermocouple probe designs in 1978. This study aims to avoid the calibration cost for each probe used in different experimental campaigns. This study is an extension of previous work by the same institute [17]. This report is selected as a validation case because its more up-to-date the test data representation is clearer. In this report, recovery correction tests were performed for ten different probe geometries, including both shielded and unshielded cases. Probe number 8 is selected as the validation case because its geometric details are more suitable to mount in high-speed and temperature environments. Geometric details of the modelled probe can be seen in Figure 2.1 The thermocouple probe comprises a type-K wire in a swaged construction with stainless steel sheath and shield [12].

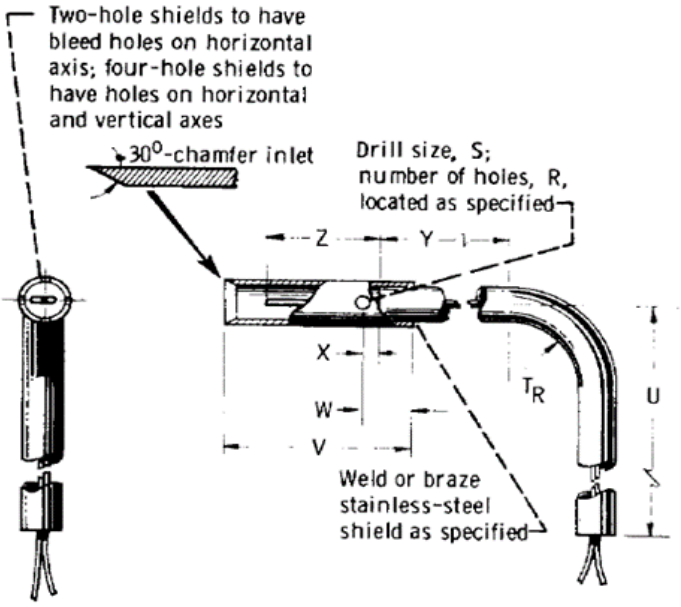

Figure 2.1: The Selected Probe Geometry for CHT Simulations [12].

The test apparatus which is designed to execute recovery correction tests consists of a plenum chamber upstream of a temperature probe, a flow nozzle accelerating flow to reach test Mach numbers, upstream and downstream control valves regulating the plenum chamber pressure and air mass flow rate passing through. With this configuration, the flow nozzle outlet Mach number can be controlled for a specific plenum chamber pressure. The total temperature of the air in the plenum chamber and the total temperature measured by the test probe which is positioned just downstream of the nozzle exit is measured separately. Additionally, a differential circuit between both measurements gives a direct output of temperature difference. With this method, the accuracy of measurements can be decreased down to ± 0.06 K [12]. No conditioning on temperature is applied because the aim of these tests it to investigate the effect of flow Mach number on recovery characteristics.

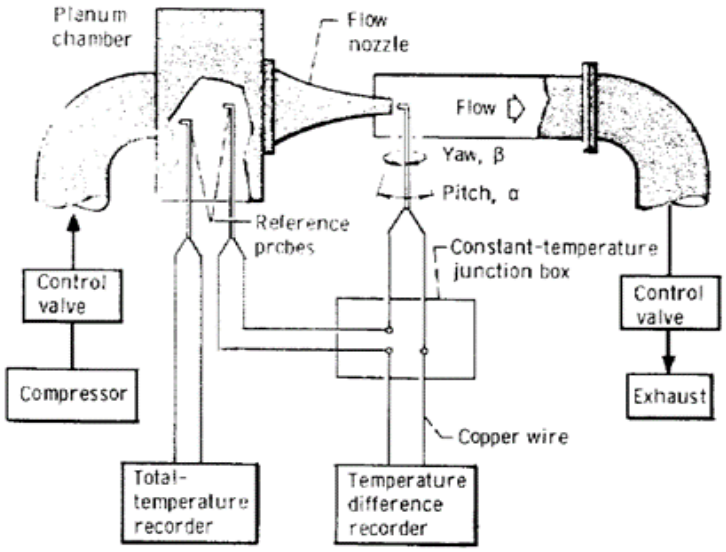

Figure 2.2: The Schematic of Recovery Correction Test Rig [12].

2.1 Numerical Methods

Fluent code was used as the solver. 3-D continuity, momentum and energy equations for each cell in fluid zones were solved simultaneously using the finite volume method until reaching an acceptable solution. For the solid regions, only the energy equation was solved. For each conservative flow variable following transport, equation 2.10 is adapted for each cell in the fluid and solid domains [18].

$$\iiint \frac{\partial \rho\varphi}{\partial t} dV + \oint \rho\varphi\vec{v}.d\vec{A} = \oint \Gamma_\varphi \nabla\varphi.d\vec{A} + \iiint S_\varphi dV \qquad (2.10)$$

Where φ is the scalar quantity for which all equation is constructed. It takes the value of 1 for the continuity equation, x, y and z velocity values for the momentum conservation equation and internal energy for the energy conservation equation. ρ is fluid density whereas $\vec{v}$ is flow velocity in vectorial form. These parameters govern the convective transport of φ between different control volumes. Γ_{φ} and $\nabla\varphi$ is the diffusion coefficient and spatial gradient of scalar quantity respectively. These values govern the diffusion of scalar quantity perpendicular to the flow direction. Lastly, S_{φ} is the source term. It is active if the scalar quantity is produced or destroyed inside the control volume [18].

Simulations were done in steady mode with a fully turbulent flow assumption. Reynolds Averaged Navier Stokes (RANS) approach with SST k-w turbulence model was used to account for turbulent shear stress effects on the flow field. In the RANS method, fluctuating terms of each flow variable are time-averaged and transport mechanisms due to turbulence are modelled as new shear stress terms. These shear stress terms are calculated using the eddy viscosity approach. SST k-w turbulence model involves a blending function which allows the application of the k-e model in freestream and the k-w model near the wall [19]. As the total temperature probe case must both solve boundary layer and freestream flow features around and inside the shield with high accuracy to be able to model the heat transfer process, SST k-w turbulence model was selected for simulations.

The pressure-based coupled algorithm is used as the calculation algorithm. In coupled algorithms, all conservation equations are solved simultaneously. The flow field is obtained using momentum equations, pressure values are corrected using velocity field and mass fluxes and then energy and other active conservation equations are solved [18].

2.2 Geometry and Fluid Domain

Probe geometry was modelled using ANSYS Design Modeler software. Probe geometry contains an elbow-to-position thermocouple wire parallel to the flow. This part wasn't modelled considering that heat conduction effects due to heat flow from the thermocouple tip to the probe stem weren't investigated in the scope of this study

and the bent section has a negligible effect on the upstream flow field around the shield.

Probe was positioned at the centre of a 150 mm diameter pipe in the model to simulate nozzle outlet flow conditions. This diameter value wasn't given in the report. Thus, this value was determined to have enough space to avoid any effect of the pipe wall boundary layer on the probe flow field. Geometry was created as a half model to reduce the computational cost. The solid part of the temperature probe on which temperature distribution will be investigated was modelled either. Generated flow and solid domains can be seen in Figure 2.3 with the boundary surfaces. All four parts of the probe (Thermocouple Wires, Potting, Sheath, Shield) with different materials were modelled as separate zones and related materials were assigned. Different zones of the temperature probe were shown in Figure 2.4.

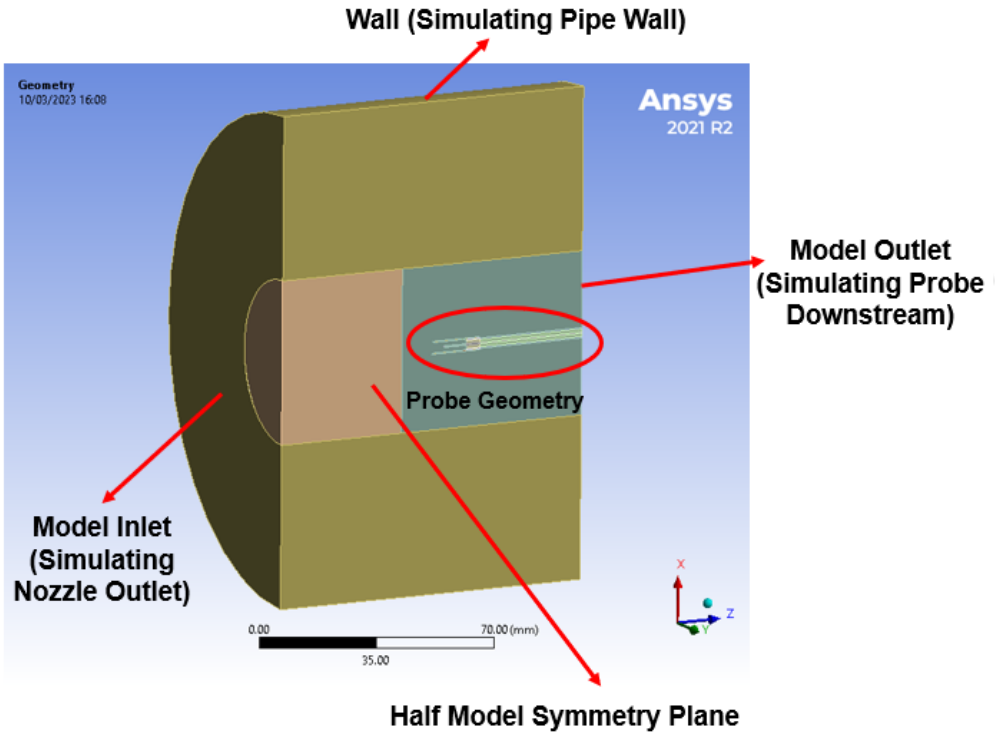

Figure 2.3: Generated Fluid and Solid Domain.

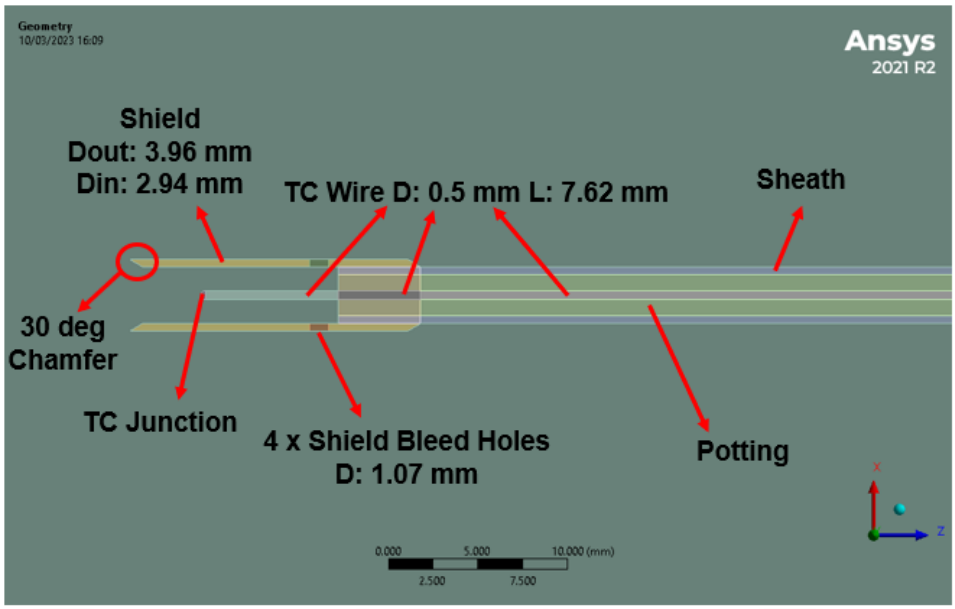

Figure 2.4: Different Zones of Modelled Temperature Probe.

2.3 Mesh Structure

Spatial discretization of the model was carried out using the Mesh module of the ANSYS software. Fluid regions far from the probe are suitable for hexahedral meshing. Fluid regions around and inside of the probe are more complex. Thus, the hexahedral mesh couldn't be applied. These parts are discretized using tetrahedral elements. Mesh is refined around the probe shield where the flow is complex due to expected flow separation on the shield's outer surface and mixing of jets discharging from bleed holes to freestream. The mesh inside of the shield is refined again to capture flow details inside of the shield. The mesh structure and refinement process were represented in Figure 2.5.

2.4 Boundary Conditions and Material Properties

The tested temperature probe was exposed to fluid flow under specific Mach number regimes. The main parameter affecting recovery characteristics is the Mach number of the flow field. Thus, the most important parameter in the analysis setup is the inlet Mach number. To set the desired inlet Mach number, the static pressure quantity defined in the pressure outlet boundary was iterated for a specific inlet pressure and temperature. The pipe wall was defined as stationary and adiabatic as the heat transfer through pipe surfaces does not affect the temperature probe. Interfaces between solid

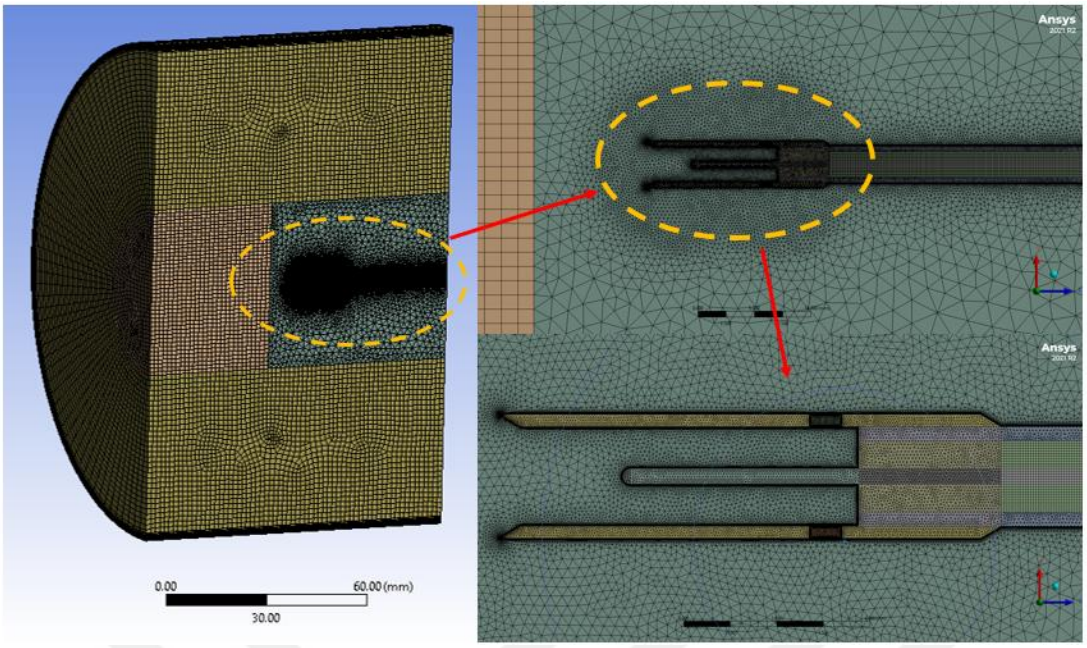

Figure 2.5: Mesh Structure of Fluid and Solid Domains.

and fluid regions were defined as "Coupled Walls" which is a boundary condition directly transferring temperature data on the first layer of the flow field to the outer boundary of the solid region [18].

As described in Figure 2.4, the temperature probe consists of different zones and these zones are made of different materials. Thermophysical properties of these materials as a function of temperature must be defined on the software for accurate simulation because high Mach number flow causes temperature gradients along the solid regions too. Thermophysical properties of density (ρ) thermal conductivity (k) and isobaric specific heat (Cp) are referenced from TPRC Data Series [20].

The thermocouple wire inside of the probe is K type whose positive leg is composed of 90% nickel, 10%chromium and the negative leg is composed of 95% nickel, 2% aluminium, 2% manganese and 1% silicon. Thus, the material properties of pure nickel are considered to be applicable.

Air is modelled as an ideal gas and its thermophysical properties of thermal conductivity (k) and isobaric specific heat (Cp) were referenced from [21]. For molecular viscosity, Sutherland's Law was used.

2.5 Mesh Dependency Study

A mesh dependency study was conducted to determine the necessary mesh size of the domain. The observed parameter during simulation runs was the thermocouple junction temperature which gives the temperature reading of all measurements if errors due to the data acquisition system are neglected.

Three meshes with 2M, 3M and 4M elements were compared. Mesh was refined for each region shown in Figure 2.5. As there is a negligible difference between 3M and 4M cases. 3M mesh size is decided to be enough in the context of this study.

2.6 Results

Three cases of 0.3, 0.6 and 0.9 Mach were solved for validation purposes of CHT methodology. The case of 0.6 M was investigated in detail to understand flow physics inside and around the probe because this case involves both low-speed and high-speed features.

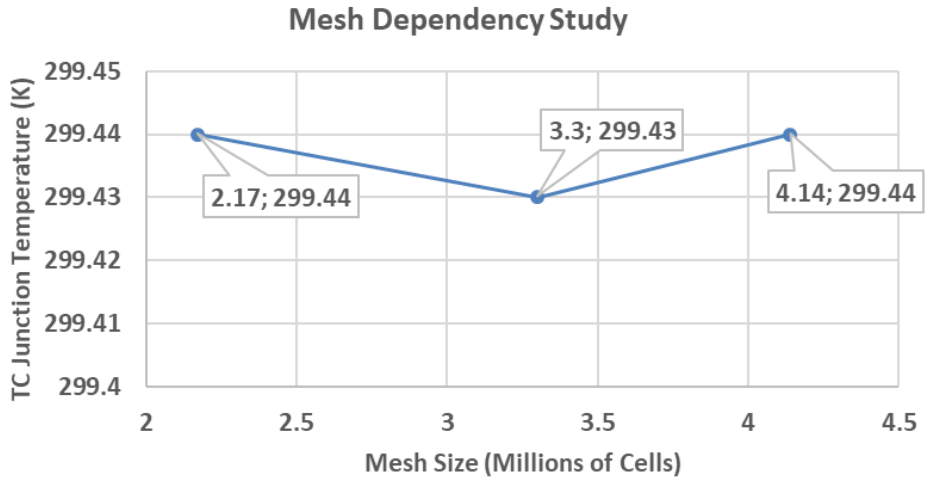

Figure 2.6: Mesh Dependency Study.

2.6.1 Flow Structures around and inside of the Total Temperature Probe

To check the validity of the CHT methodology, 0.3, 0.6, and 0.9 Mach cases were simulated with an inlet temperature of 300 K and inlet pressure of 1 atm. Outlet static pressure was iterated until matching the inlet Mach number with the test condition. Flow Mach number distribution on the symmetry plane is presented in Fig. 2.7. Mach number was observed to decrease down to 0.2 M inside of the shield for the case of 0.6 M due to the limitation of shield inlet mass flow from bleed holes whose total area

is half of shield inlet area. This was the main aim of probe design and it seems to be accomplished at some degree. With the reduction of the Mach number inside the shield, the flow static temperature rose and the difference between total and static temperatures of flow decreased. This led to a thinner boundary layer with lower velocity and temperature gradients and thermal diffusion.

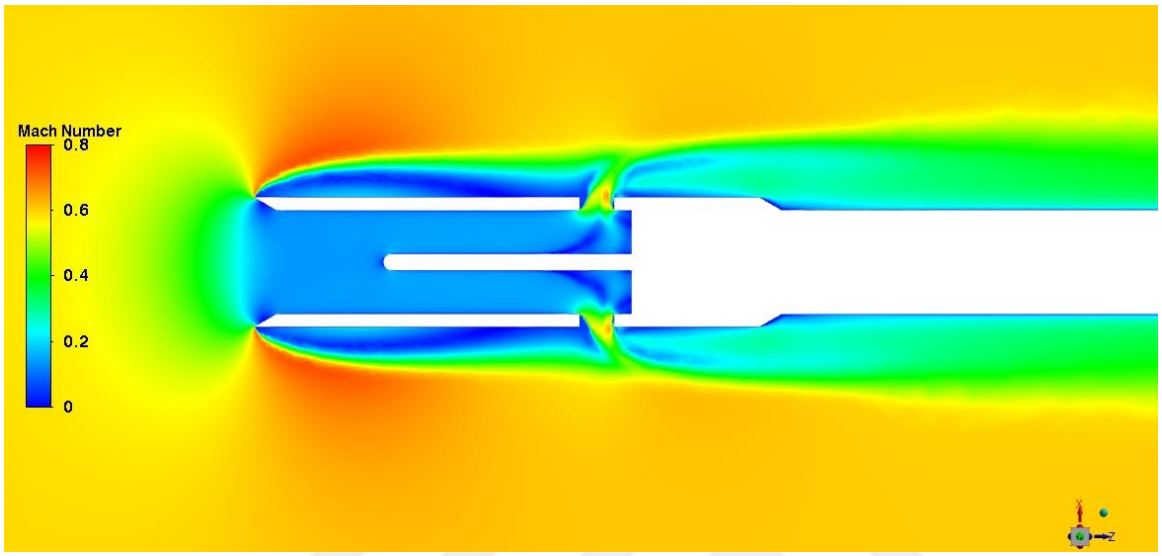

Figure 2.7: Mach Number Distribution on Symmetry Plane for 0.6 M Case.

Velocity vectors are presented in Figure 2.8. No flow separation was observed on the shield inlet. On the outer surface of the probe shield, a large separation region occurred as expected due to the sharp corner. Flow reattached before reaching bleed holes and this separation region didn't cause any further limitation on the mass flow rate inside of the shield.

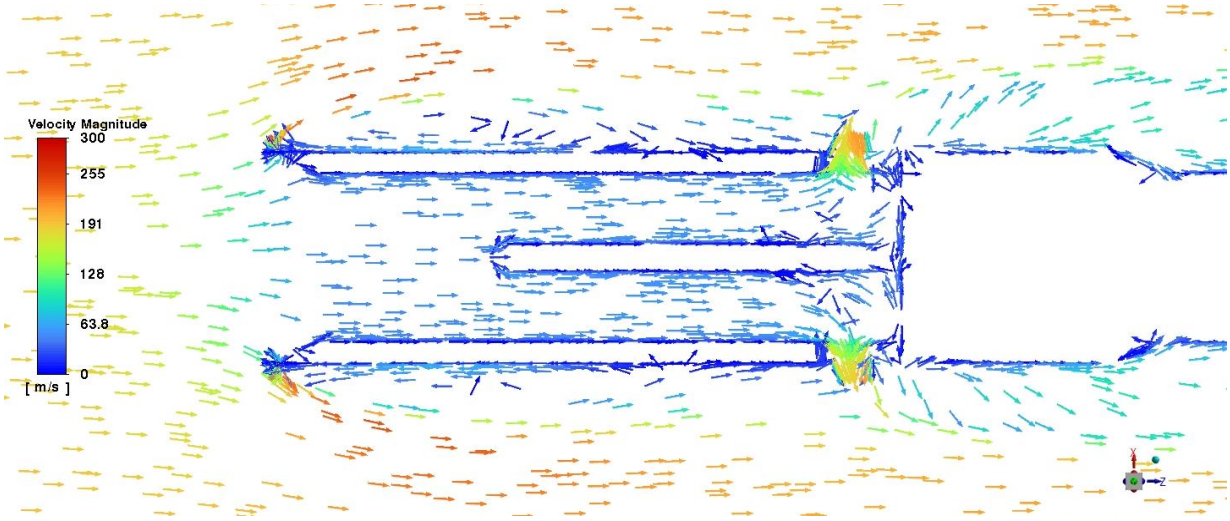

Figure 2.8: Velocity Vector Field on Symmetry Plane at 0.6 M Case.

As presented in Fig. 2.9, the flow total temperature decreased on the probe surfaces. This is impossible if we think in terms of the energy conservation principle because boundary walls were defined adiabatic, and no work interaction occurs on the flow field.

To understand this phenomenon the static temperature contour was drawn in Fig. 2.10, regions of lower total temperature present higher static temperature values in contrast. From this observation, it can be said that the heat is conducted from high static temperature areas to lower ones along the flow field. Due to this energy transfer, the total temperature of some local areas decreases while it increases in different areas. The total energy is conserved but the distribution of energy becomes non-uniform due to the presence of probe geometry. This non-uniformity reflects itself as a different boundary condition on the solid-fluid interface different from the freestream flow total temperature. That is the source of the recovery error.

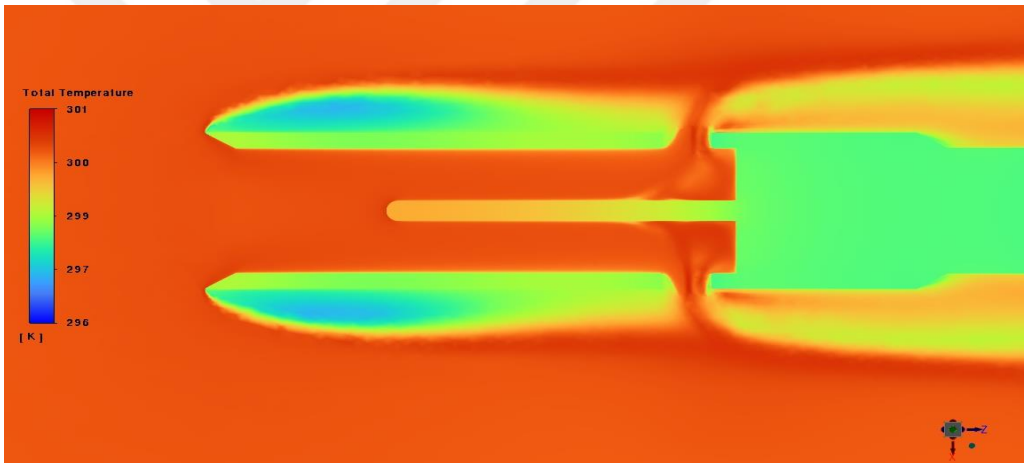

Figure 2.9: Static Temperature Distribution on Symmetry Plane at 0.6 M Case.

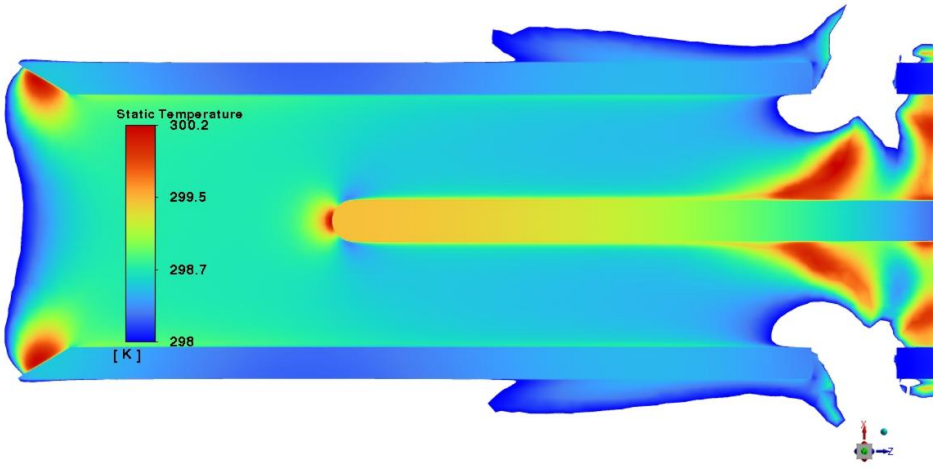

Figure 2.10: Static Temperature Distribution inside Shield on Symmetry Plane at 0.6 M Case.

2.6.2 Comparison of CHT Results with Experimental Data

In Table 2.1 and Figure 2.11, T_j and r values and distributions are presented as a comparison of CHT and experimental data. The experimental data comes from the recovery factor data of [12]. For the cases of 0.6 and 0.9 Mach difference in recovery correction factor is less than %0.1 between CHT and experiments, whereas for the case of 0.3 Mach difference is greater than %1.5. This is thought to be because of low dynamic temperature value at such a low speed and a very minor temperature difference of 0.1 K causes a considerable deviation.

Table 2.1: Comparison of T_j and r Values in CHT and Experiment

CHT and Experimental Data Comparison (1 bar, 300 K)			
	0.3 M	0.6 M	0.9 M
T_j CHT	299.79	299.44	299.02
T_j Exp.	299.7	299.4	299.1
r CHT	0.960	0.972	0.977
r Exp.	0.943	0.970	0.978

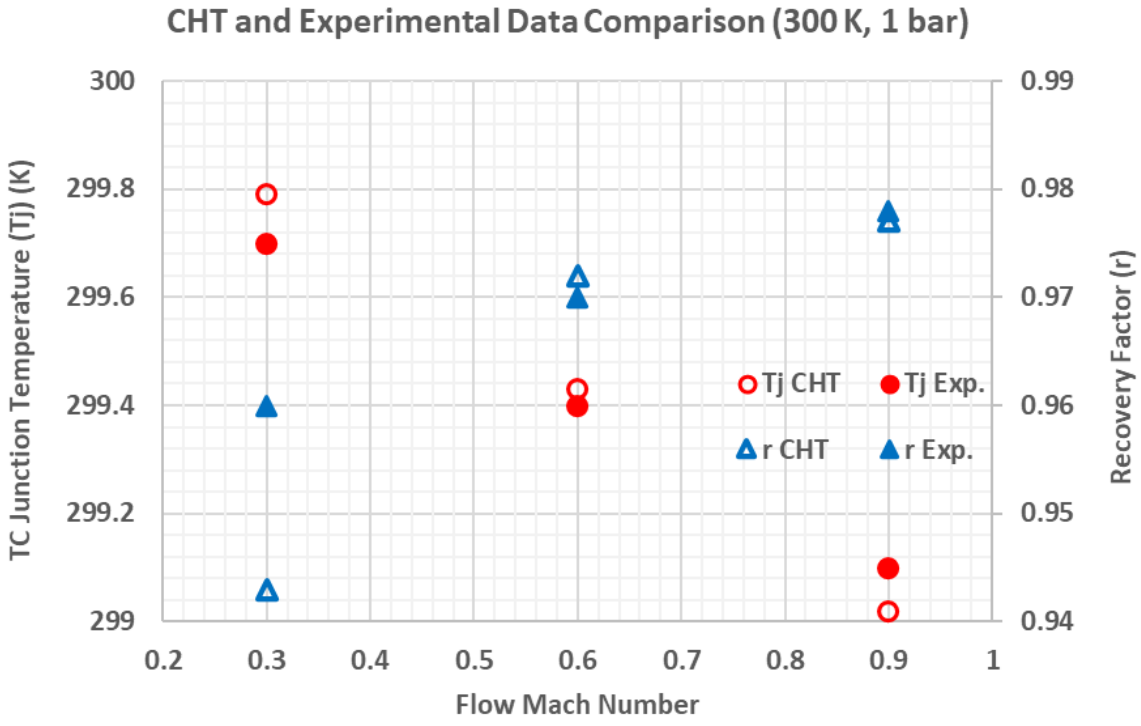

Figure 2.11: T_j and r Distributions in CHT and Experiments.

3. PARAMETRIC STUDY

3.1 Flow Angle

In many conditions, flow isn't purely one-dimensional, and it isn't easy to guess the flow direction exactly. Thus, a measurement probe should be capable of measuring flow parameters correctly despite variations in upstream flow angle. To investigate the capability of probe geometry, simulations with varying flow angles in the radial direction between 0-30 degrees were done. Two different probe geometries having straight tips (ST) and conical tips (CT) were also investigated to examine the effect of 30 degrees chamfer at the shield inlet. The probe geometry model with a straight tip is presented in Figure 3.1.

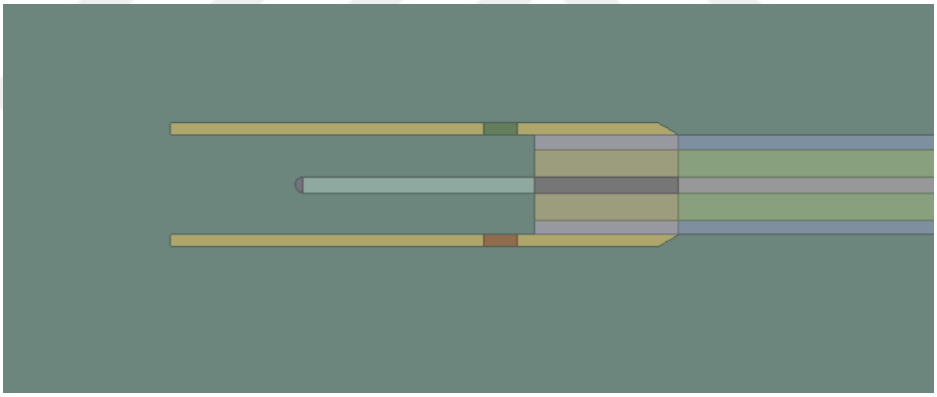

Figure 3.1: Straight Tip Probe Model.

Fluent code allows the definition of flow angle at the inlet boundary. Flow angle was defined at the inlet of the solution domain and outlet static pressure was iterated to match the required inlet Mach number. Flow vectors for the ST probe for 0 flow angle condition are presented in Fig 3.2. Small vortex regions were observed to dissipate in the inlet region of the shield and the TC junction is exposed to a streamlined flow field.

Velocity vectors of 30 degrees condition for ST and CT probes are presented in Fig. 3.3 and 3.4 respectively. Flow separation occurring on the shield inlet was observed to interact with the thermocouple junction in both conditions, this phenomenon may cause extra deviation of TC junction temperature.

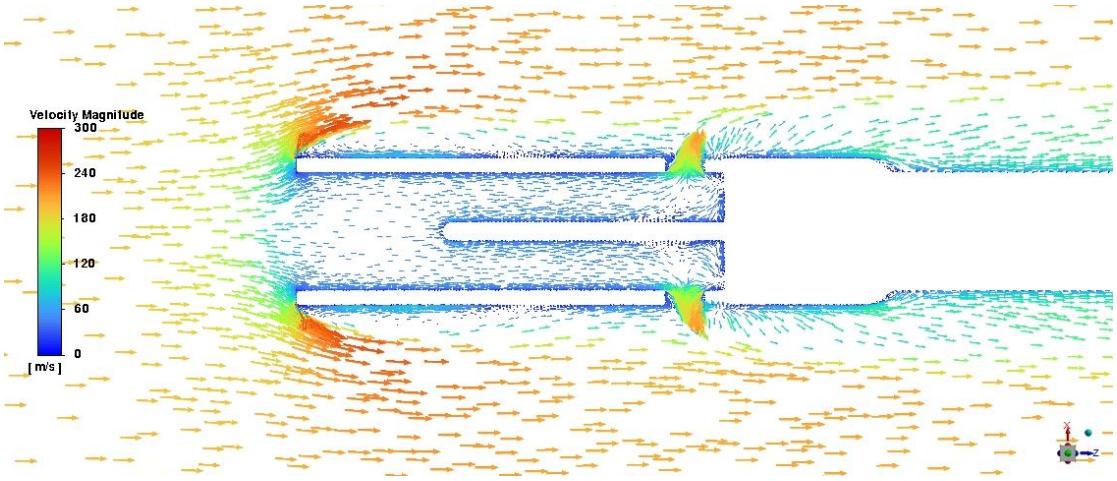

Figure 3.2: Velocity Vector Field Around and Inside of ST Total Temperature Probe on Symmetry Plane at 0.6 M Case for 0 Flow Angle.

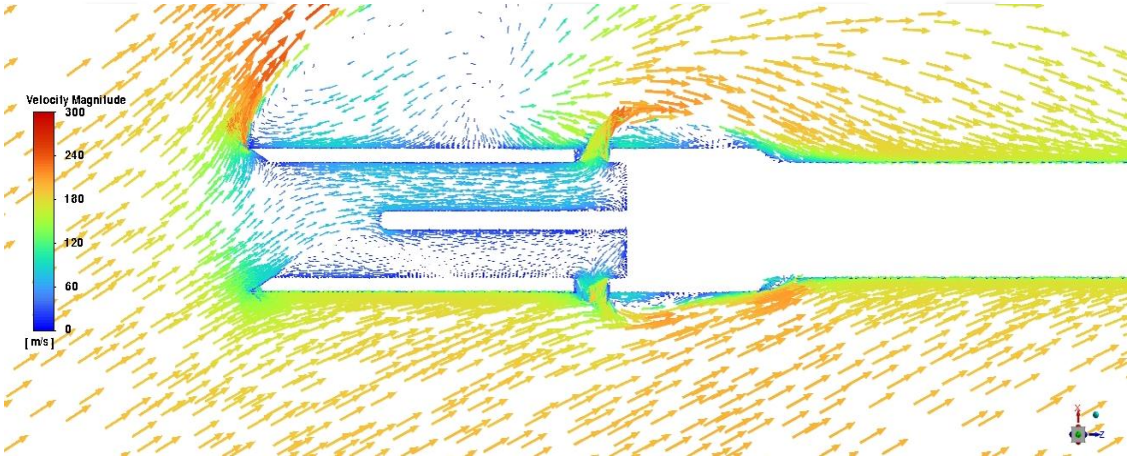

Figure 3.3: Velocity Vector Field Around and Inside of CT Total Temperature Probe on Symmetry Plane at 0.6 M Case for 30 deg Flow Angle.

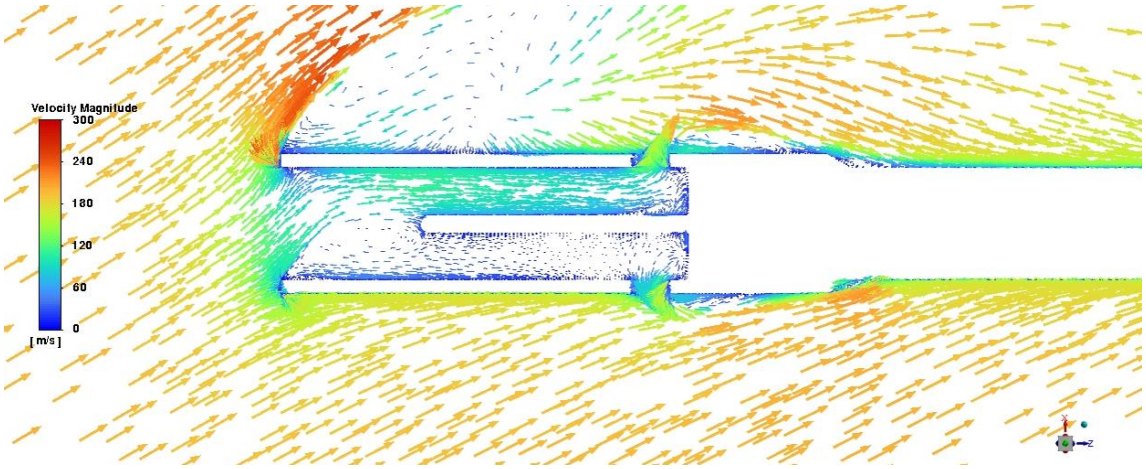

Figure 3.4: Velocity Vector Field Around and Inside of ST Total Temperature Probe on Symmetry Plane at 0.6 M Case for 30 deg Flow Angle.

In Table 3.1 and Figure 3.5, T_j and r values and distributions are presented. Until 20 deg flow angle variation in r is less than %1 so the probe geometry can be thought of as resistant to flow angle values up to 20 deg. In the 30 deg case, the CT probe performs much better than the ST one as the ST probe's r value deviates more than %2.5. It can be concluded that a CT probe is advised if flow angle uncertainty is too high in the specific case.

Table 3.1: T_j and r Values under Flow Angle Variation for ST and CT Probes

Flow Angle Sensitivity Study (0.6 M, 1 bar, 300 K inlet)				
	0 deg Flow Angle	10 deg Flow Angle	20 deg Flow Angle	30 deg Flow Angle
T_j – ST	299.42	299.36	299.32	298.87
T_j – CT	299.43	299.34	299.28	299.15
r – ST	0.971	0.968	0.966	0.944
r – CT	0.972	0.964	0.962	0.958

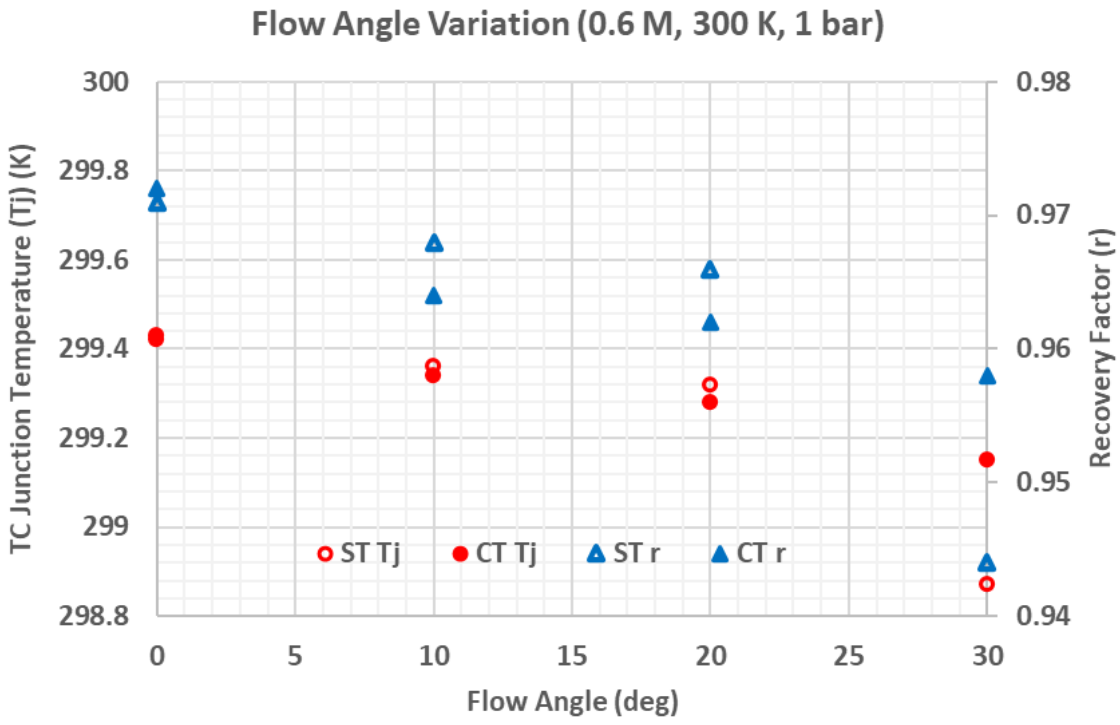

Figure 3.5: T_j and r Distribution under Flow Angle Variation for ST and CT Probes at 0.6 M Case

3.2 Area Ratio

The ratio between the shield inlet surface area and the total area of bleed holes is one of the primary parameters of a total temperature probe design as described in Section 1.4. To make a more accurate total temperature measurement, the flow should be decelerated to an acceptable range without any energy loss. This is accomplished using the bleed hole strategy. Bleed holes are positioned downstream of the thermocouple junction and shield inlet. Bleed holes function like an atmospheric jet. Inside bleed holes are pressurized taking energy from upstream flow and flow discharges to an environment whose pressure is static pressure of flowing fluid at a certain Mach number. Thus, the mass flow rate of flow entering is set from bleed holes. Usually, the bleed hole total area is dimensioned to be less than the shield inlet surface but in some conditions in which error sources due to conduction and radiation are present, decreasing velocity may give negative results because heat transfer due to convection decreases and a greater temperature difference must be present to create thermal equilibrium.

In CHT simulations, the validity of this theoretical approach was investigated. Cases with an area ratio from 0.5 to 4 were simulated. Mach number distributions and measurement errors were discussed.

Figures 3.6 and 3.7. Mach number distributions for AR 0.5 and 4 cases are presented respectively. As expected, for the AR- 0.5 case Mach number values are much greater. Although the bleed hole total area is greater than the shield inlet area in AR 0.5 case. Mach number values inside of shield are less than freestream values. This is because of that flow turning on the inlet of bleed holes causes a vena contracta and blockage of some of the flow area of the bleed holes. This phenomenon causes a less effective flow area than the total area of bleed holes.

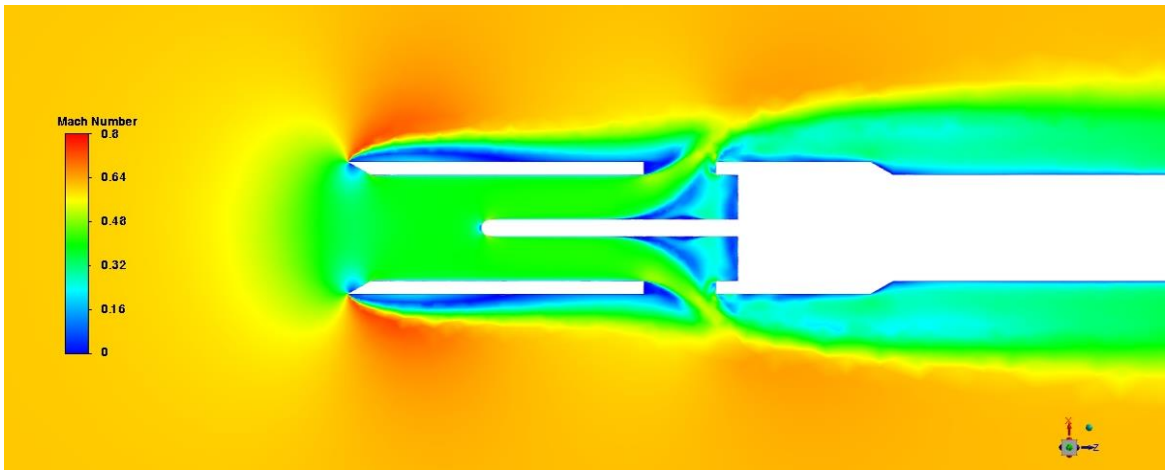

Figure 3.6: Mach Number Distribution on Symmetry Plane for AR-0.5

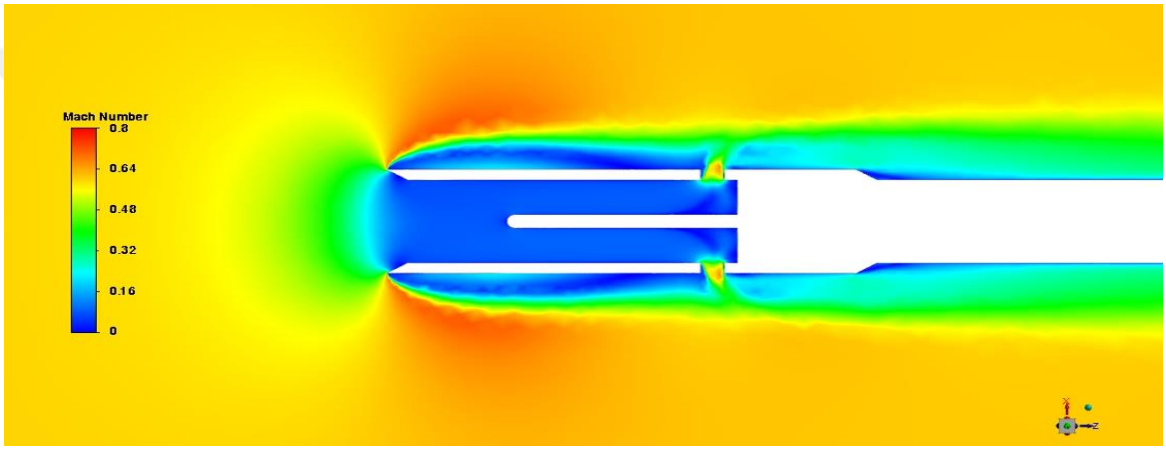

Figure 3.7: Mach Number Distribution on Symmetry Plane for AR-4.

In Table 3.2 and Figure 3.8, T_j and r values and distributions are presented. There is no significant change between AR-4 and 2 so it is advised to increase the area ratio up to 2. As seen in the table recovery factor gets down to 0.914 for AR 0.5 and temperature deviation increases considerably. So experimentalists must be very careful while selecting an AR less than 2. This may be beneficial if radiation and conduction error mechanisms are present but will cause big deviations due to the recovery error.

Table 3.2: T_j and r Values under Area Ratio Variation

Hole Area Ratio (Inlet to Bleed) Sensitivity Study (0.6 M, 1 bar, 300 K inlet)				
	AR-4	AR-2	AR-1	AR-0.5
T_j	299.49	299.43	298.92	298.27
r	0.975	0.972	0.946	0.914

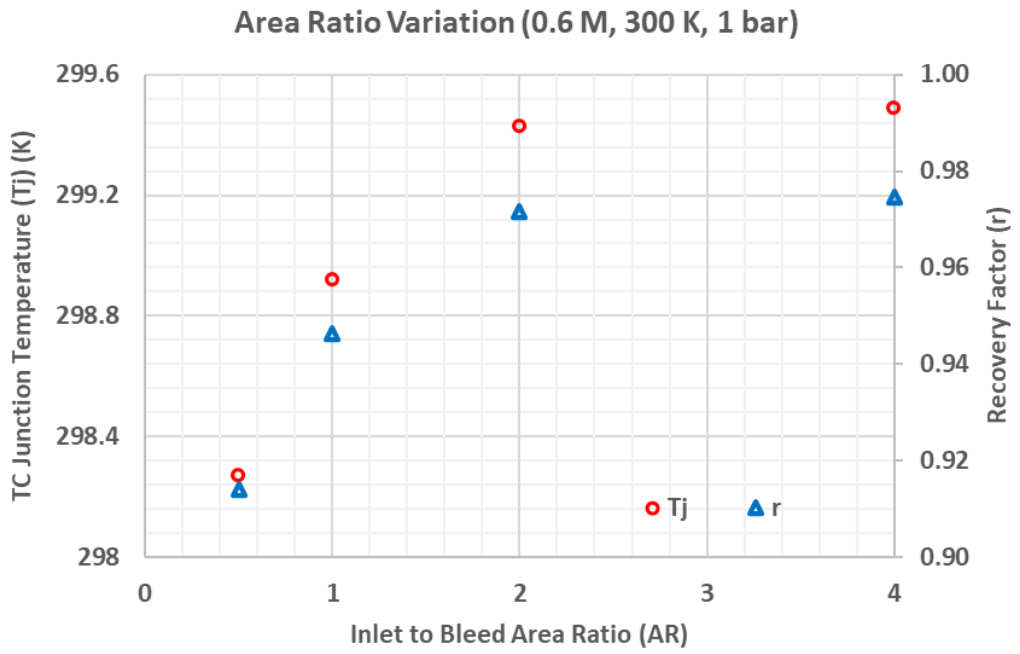

Figure 3.8: T_j and r Distribution under Area Ratio Variation

3.3 Temperature

The effect of inlet temperature was investigated for two different Mach number regimes in the range of 200 K-1500 K. In Figures 3.9 and 3.10, Mach number distributions are presented for 200 K and 1500 K cases respectively. Mach number distributions for both cases are very similar so it can be deduced that temperature variation doesn't have a great impact on flow characteristics inside the shield. In Table 3.3 and Figure 3.11, T_j and r values and distributions are presented. Recovery values are greater for higher Mach numbers as expected. The recovery factor was observed to increase up to 1000 K and then started to decrease. Reynolds number (Re) whose characteristic length is TC junction diameter is in a trend of decrease due to the reduction of density at higher temperatures. No direct relation between Re was observed. This is thought to be because that Re doesn't change with a big order of magnitude in this range. The explanation of this phenomenon is related to the other dimensionless number affecting the boundary layer. characteristics, the Prandtl number (Pr). The Prandtl number is a thermophysical property and can be expressed as a function of static temperature. As seen on the secondary axis of Figure 3.11; from 200 K to 1000 K, Prandtl number is in a trend of rise which means flow becomes thermally

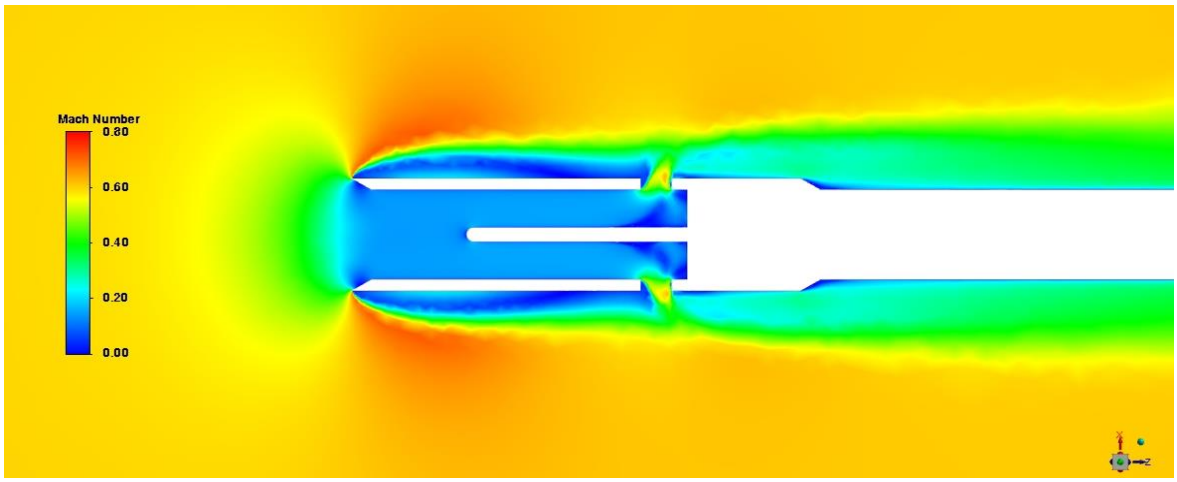

Figure 3.9: Mach Number Distribution for 200 K Flow Total Temperature

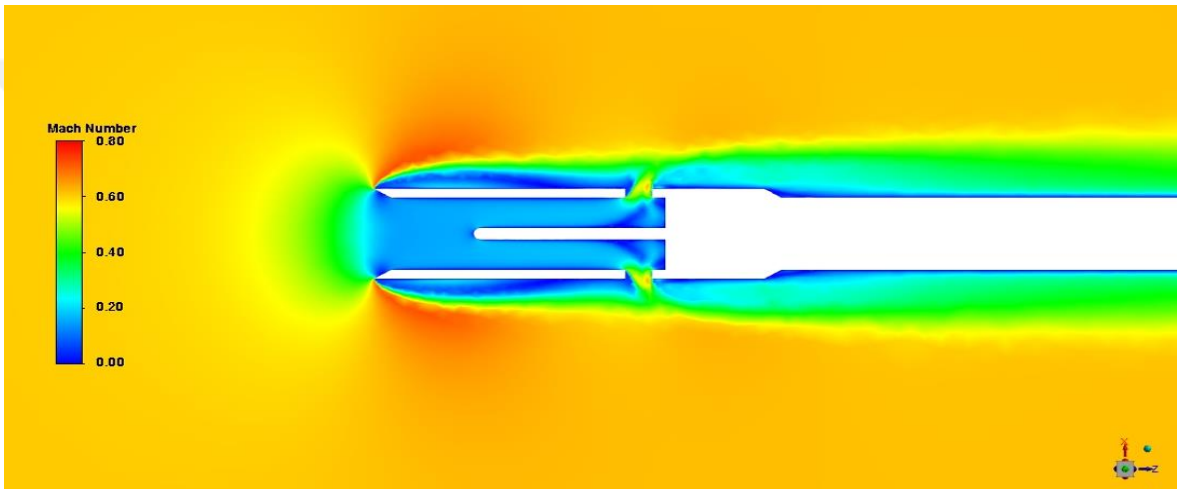

Figure 3.10: Mach Number Distribution for 1500 K Flow Total Temperature

less diffusive than momentum and the temperature of the first layer on the wall becomes closer to the flow total temperature. At about 1000 K, the Prandtl number reaches a local maximum and starts to decrease. This is a sign of more thermal diffusivity resulting in a greater temperature gradient in the boundary layer and a lower first-layer temperature. This phenomenon explains the reduction of r between 1000 K and 1500 K.

Table 3.3: T_j and r Values under Temperature Variation

Inlet Temperature Sensitivity Study (0.6 & 0.3 M, 1 bar)					
	200 K	300 K	500 K	1000 K	1500 K
T_j - 0.6 M	199.62	299.44	499.19	998.71	1497.9
r - 0.6 M	0.972	0.972	0.975	0.978	0.973
Re - 0.6 M	9652	5993	3198	1340	818
Pr - 0.6 M	0.740	0.707	0.687	0.704	0.458
T_j - 0.3 M	199.86	299.79	499.70	999.53	1499.22
r - 0.3 M	0.960	0.961	0.965	0.969	0.962
Re - 0.3 M	5312	3285	1749	737	451
Pr - 0.3 M	0.735	0.703	0.687	0.701	0.372

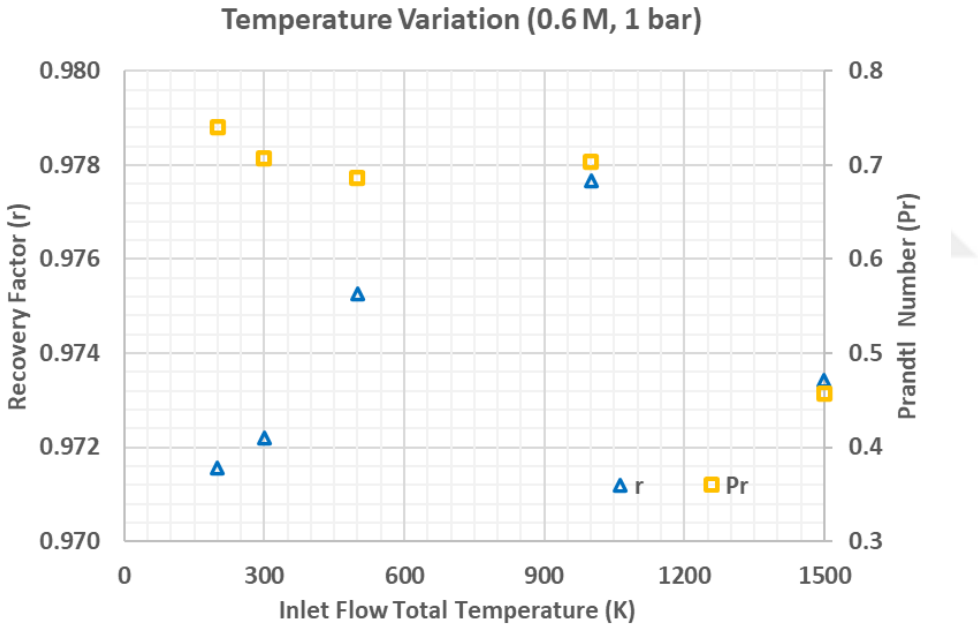

Figure 3.11: r Distribution under Temperature Variation

3.4 Pressure

The effect of inlet pressure on measurement accuracy was investigated for two different Mach number regimes in the range of 0.2 bar-10 bar covering a range of vacuum to aero-engine compressor representative pressure values. In Figures 3.12 and 3.13, Mach number distributions are presented for 0.2 bar and 10 bar cases respectively. Mach number distributions for both cases are very similar so it can be

deduced that pressure variation doesn't have a great impact on flow characteristics. In table 3.4 and Figure 3.14, T_j and r values and distributions are presented. Recovery values follow a similar trend with the temperature case in the context of Mach number variation. Reynolds number based on TC wire length constantly increased with substantial amounts. Thus, it is the most dominant parameter on boundary layer shape for this case and higher Re results in thinner BL and greater recovery values.

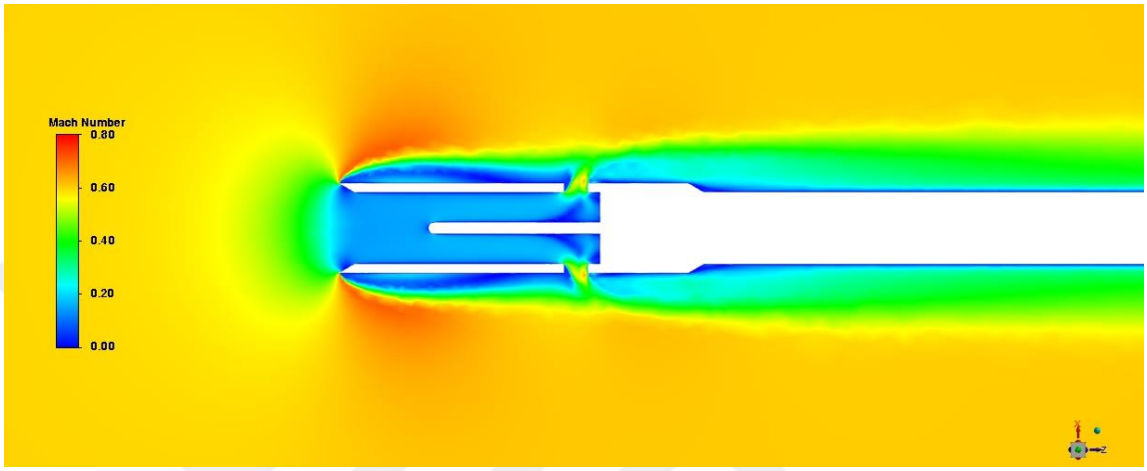

Figure 3.12: Mach Number Distribution for 0.2 bar Flow Total Pressure

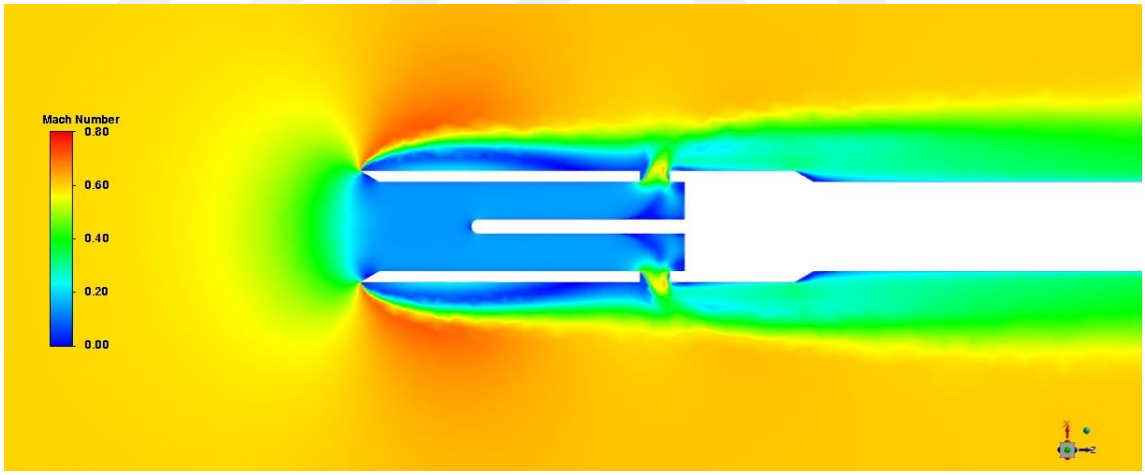

Figure 3.13: Mach Number Distribution for 10 bar Flow Total Pressure

Table 3.4: T_j and r Values under Pressure Variation

Inlet Pressure Sensitivity Study (0.6 & 0.3 M, 300 K)				
	0.2 bar	1 bar	3 bar	10 bar
T_j - 0.6 M	298.88	299.44	299.67	299.81
r - 0.6 M	0.944	0.972	0.984	0.991
Re – 0.6 M	1183	5993	17745	59150
T_j - 0.3 M	299.63	299.79	299.87	299.93
r - 0.3 M	0.930	0.960	0.975	0.987
Re – 0.3 M	649	3288	9735	32449

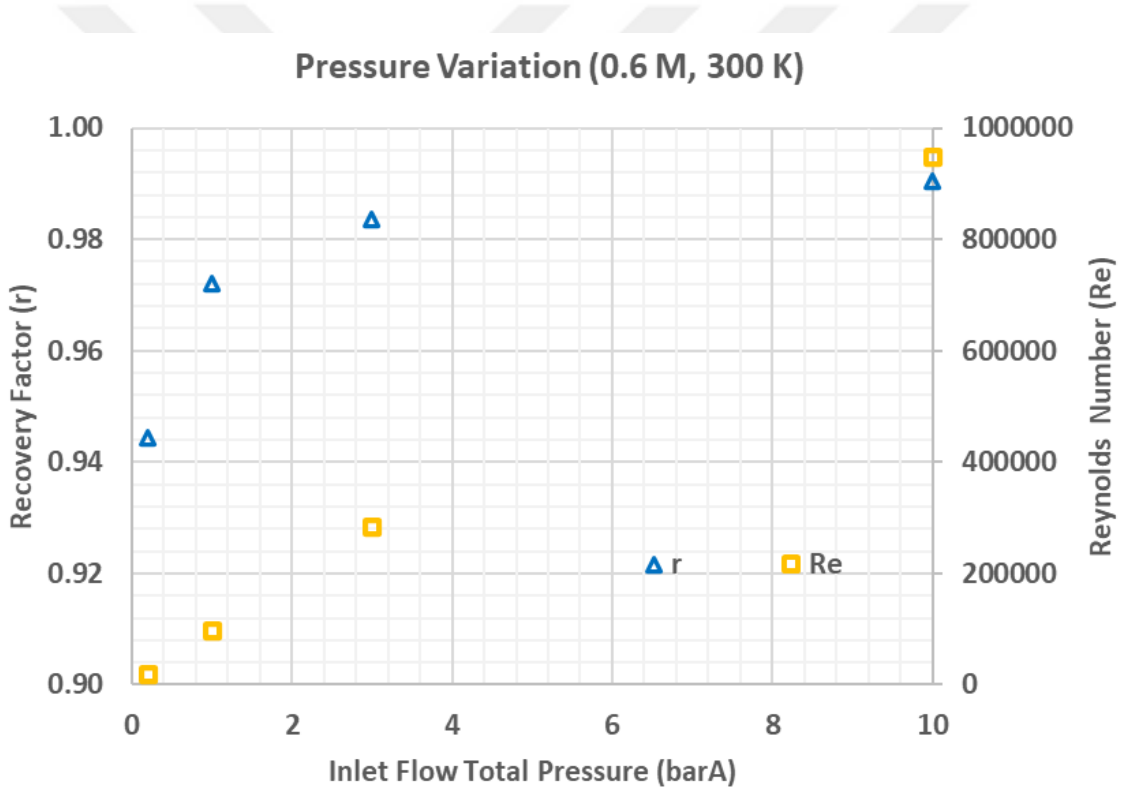

Figure 3.14: r Distribution under Pressure Variation

4. THERMAL MODELLING

CHT simulations performed until now were carried out in an environment in which no other thermal boundary condition exists. When solid temperatures around the probe deviates considerably from the flow total temperature, errors due to thermal conduction and radiation may occur. To be able to model possible errors, firstly convective heat transfer inside and around of shield will be modelled. Then, conduction and radiation errors will be calculated using basic heat transfer theory.

4.1 Determination of Heat Transfer Coefficient

Heat transfer inside of the temperature probe's shield can be modelled as an annular pipe where thermocouple wires constitute the inner body and the shield constitutes the outer body. The flow passes through TC wires' outer surface and shields' inner surface exchanging heat with both surfaces. This heat exchange occurs in convective mode. Thus, the heat transfer coefficient (HTC) for each surface can be calculated using relevant correlations.

For turbulent flow in an annular pipe, following the Gnielinski equation is advised for Nusselt number calculation [22].

$$Nu = \frac{\left(\frac{f}{8}\right)(Re - 1000)Pr}{1 + 12.7\sqrt{\left(\frac{f}{8}\right)}\left(Pr^{2/3} - 1\right)} \tag{4.1}$$

Where f is the friction factor, Re and Pr are Reynolds and Prandtl numbers of flow inside the shield. The characteristic length of Re is the hydraulic diameter of the shield.

As seen from equation 4.1, three unknowns must be determined for the calculation of the Nusselt number which will lead to the determination of the HTC. When the measurement performance of a probe is desired to be characterized, one knows

freestream flow conditions which include velocity, temperature and pressure. Inside a shield, these parameters change to increase the measurement performance of the probe as described in Section 1.4.1. This process must be modelled to calculate HTC just using known parameters to have a general model.

To model flow conditions inside a shield, a strategy derived from the recommendations of [3] will be applied. As seen from the static pressure contour of Fig. 4.1 for the case of 0.6 M, static pressure at the discharge area of bleed holes is about the free stream pressure of the flow and static pressure inside of the shield is about the free stream total pressure. As the ratio between these two pressure values causes the Mach number of flow to be equal to the freestream one, Mach numbers at bleed holes will be taken as equal to the freestream one and the mass flow rate will be calculated. Then, the Mach number at the shield inlet will be calculated using the principle of mass conservation at steady conditions. After the determination of the shield inlet Mach number, relevant flow parameters for the determination of Nu can be calculated using the basic fluid mechanics relations.

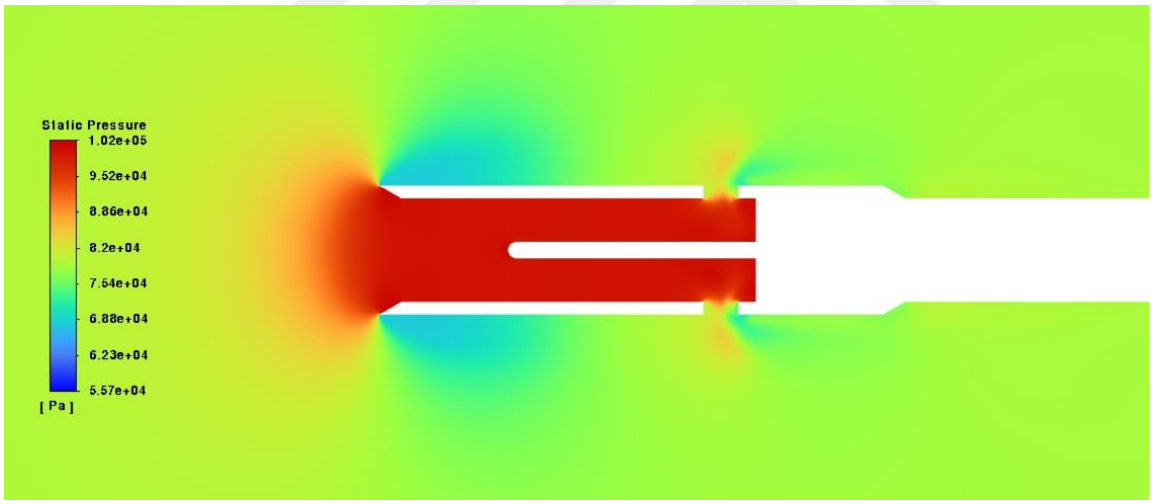

Figure 4.1: Static Pressure Distribution on Symmetry Plane for 0.6 M Case.

To calculate the shield inlet Mach number, an iterative scheme is needed. A guess for the Mach number is made and then the mass flow rate calculated with this guess is compared to the one calculated using bleed holes.

The mass flow rate passing through an area can be calculated with the following equation.

$$\dot{m} = \frac{AP_t}{\sqrt{T_T}}\sqrt{\frac{\gamma}{R}}M\left(1+\frac{\gamma-1}{2}M^2\right)^{\frac{-(\gamma+1)}{2(\gamma-1)}} \tag{4.2}$$

If the Mach number is known, static temperature and pressure can be calculated using the following isentropic relations,

$$T_S = T_T(1+\frac{\gamma-1}{2}M^2)^{-1} \tag{4.3}$$

$$P_S = P_T(1+\frac{\gamma-1}{2}M^2)^{-\frac{\gamma-1}{\gamma}} \tag{4.4}$$

After the determination of thermodynamic parameters of pressure and temperature, the density and velocity of flow can be determined with the following equations,

$$\rho = \frac{P_S}{RT_S} \tag{4.5}$$

$$V = Ma = M\sqrt{\gamma RT_S} \tag{4.6}$$

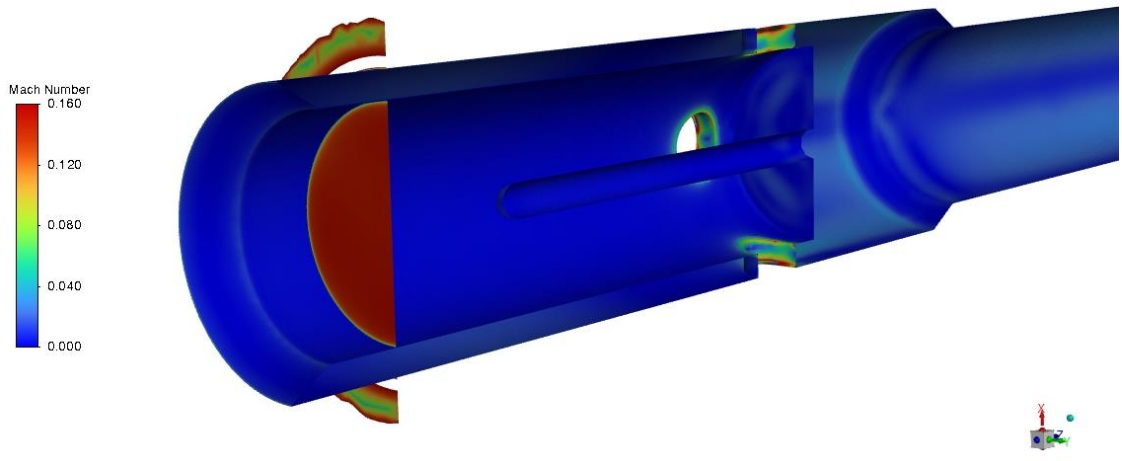

Figure 4.2: Mach Number Distribution at Shield Inlet for 0.6 M Case.

As seen in Fig. 4.3, shield inlet Mach numbers in CHT are less than the calculation values. This can be explained by the fact that the whole bleed hole area isn't the

effective area of flow. Thus, a discharge coefficient (C_d) must be defined. A C_d the curve was created for varying pressure ratios and embedded into the calculation methodology in Fig. 4.4. The C_d curve is defined as a function of the total to static pressure ratio on the bleed holes. Shield inlet flow parameters were calculated after the C_d correction had been applied to the calculated mass flow rate.

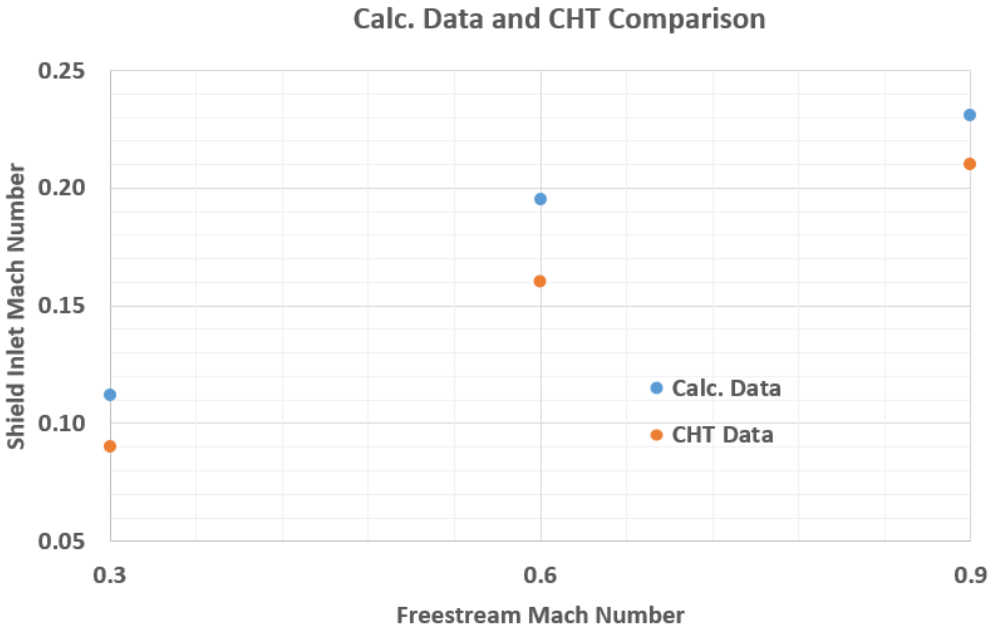

Figure 4.3: Shield Inlet Mach Number in CHT and Calc. Methodology

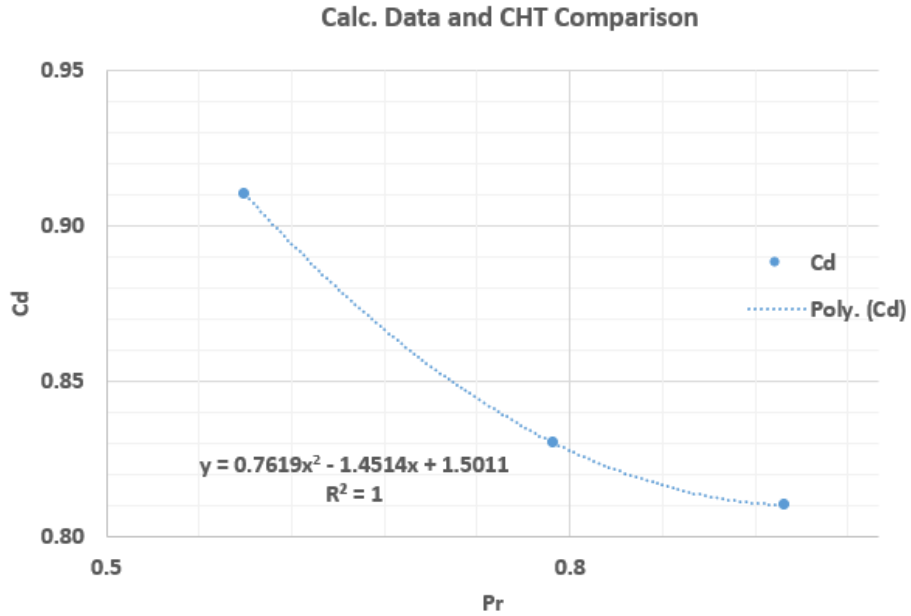

Figure 4.4: C_d Curve for Varying Pressure Ratio.

4.2 Conduction Error Modelling

As was explained in Section 1.4.2, conduction error arises due to heat flow between TC junction and solid regions. In a real situation, the total temperature probe is mounted to a solid region and likely, the temperature of this probe mount region is different from the flow total temperature. The temperature of the flow field may also vary spatially so temperature gradients occur along the probe body. As the modelling of whole this process is so complex, carrying out a sensitivity study seemed more practical. In this study, TC wire is assumed as a one-dimensional fin and the point TC wire is mounted to the probe body is taken as a boundary condition affecting TC junction temperature. The effect of TC wire mount region temperature on TC junction temperature was investigated.

Using the heat transfer theory of fins assuming an adiabatic tip, the following equation is derived [3].

$$T_j = T_t - \frac{T_t - T_M}{cosh\left[L\left(\frac{4h_c}{Dk_s}\right)^{\frac{1}{2}}\right]} \tag{4.7}$$

Where T_t, T_j are flow total temperature and junction temperature respectively. T_M is the solid temperature where the thermocouple wire is mounted to the probe strut, L is the length of the thermocouple wire, D is the diameter of the thermocouple wire, k_s is the thermal conductivity of TC wire material, h_c is the heat transfer coefficient inside the shield. As T_t, L, D and k_s are apriori known parameters and h_c is calculated using the methodology explained in Section 4.1. T_j can be calculated using this explicit equation for varying T_M for a specific geometry and flow condition.

The sensitivity of temperature probe design to conduction error was investigated for 0.6 Mach number regime in Fig. 4.5, 4.6 and 4.7 for different mount temperatures of 990 K, 970 K and 950 K respectively. As shown in Table 4.1, the effect of the Mach number effect on conduction error was observed to be nearly negligible. This can be explained by the fact that the shield inlet velocities are in a narrow range despite variations in free stream velocities due to the mass flow controlling nature of the bleed hole design. Flow temperature and pressure were chosen as 1000 K and 5 bar

respectively. These values represent possible conditions at an engine hot section where conduction error comes into play. Different probe geometries whose distinctive feature is the area ratio between bleed holes and shield inlet area were investigated either. When the mount temperature was set as 950 K, deviations up to 20 K which corresponds to a %2 error for an AR of 0.25 was observed. Thus, the experimentalists should carefully investigate flow conditions at the measurement location to avoid such errors.

Table 4.1: Conduction Error Values for Varying *Tm*.

Conduction Error Values (0.6 M, 5 bar, 1000 K)			
	AR-1	AR-2	AR-4
T_M - 990 K (0.6 M)	998.75	997.02	995.89
T_M - 990 K (0.3 M)	998.78	997.07	995.95
T_M - 970 K (0.6 M)	996.26	991.06	987.67
T_M - 970 K (0.3 M)	996.35	991.2	987.84
T_M - 950 K (0.6 M)	993.77	985.6	979.44
T_M - 950 K (0.3 M)	993.91	985.84	979.74

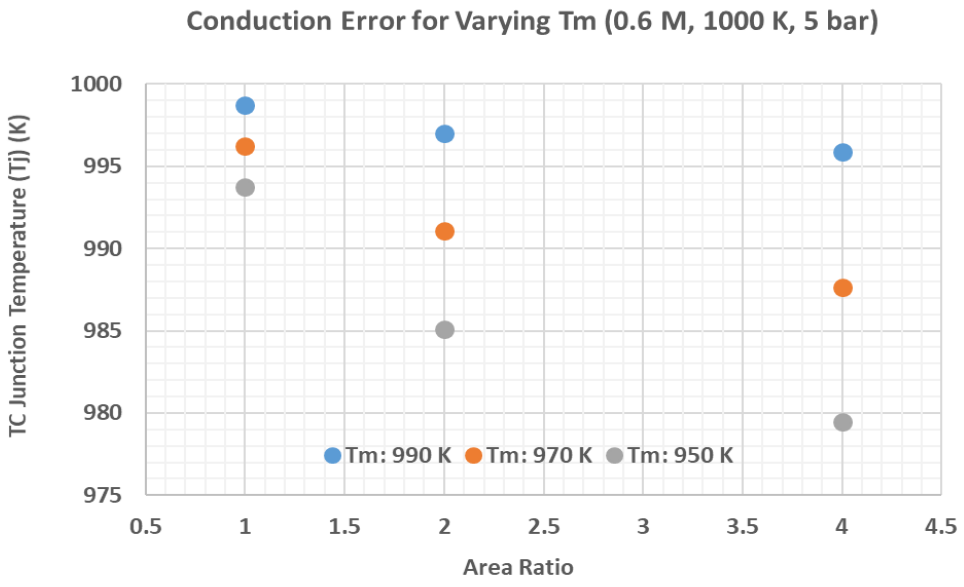

Figure 4.5: Conduction Error Distribution for Varying *Tm* at 0.6 M Case.

The effect of TC wire length on T_j was also investigated in Fig. 4.8 for 0.6 M, 5 bar and 1000 K flow conditions. Increasing wire length up to 16 seems to provide considerable gain and decrease the dependency of conduction error to shield AR but an L/D ratio up to 15 is advised in many references as explained in section 1.4.2 due to the mechanical concerns. A wire length of 16 corresponds to an L/D of 32 for a 0.5 mm diameter TC wire. Thus, increasing the L/D ratio must be carefully analysed before application considering the flow conditions and susceptibility to mechanical damage.

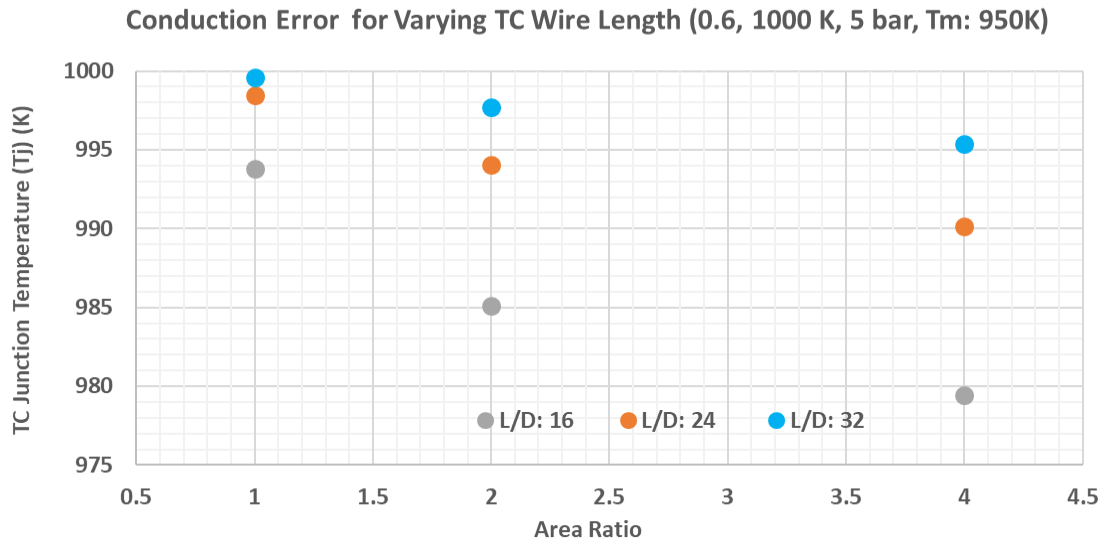

Figure 4.6: Conduction Error Distribution for Varying TC Wire Length.

4.3 Radiation Error Modelling

As was explained in Section 1.4.3, radiation error arises due to heat flow between the TC junction and solid regions. In a real situation, the total temperature probe is mounted inside of the machine and likely, there are solid regions around the probe whose temperature takes different values from the flow total temperature. The TC junction interacts with all these regions if they are in its line of sight. As the modelling of whole this process is so complex, carrying out a sensitivity study seemed more practical. In this study, the total temperature probe is considered to be mounted at the centre of a cylindrical duct whose wall temperature is different from the flow total temperature. In such a configuration, the TC wire becomes fully enclosed by the duct wall. As the total temperature probe contains a shield geometry surrounding the TC wire. TC wire also should be modelled as a body enclosed by a different one. Thus, a

heat transfer network occurs between these three elements (Duct Wall, Shield and TC wire).

For shield temperature,

$$Q_{conv1} + Q_{conv2} + Q_{rad1} + Q_{rad2} = 0 \tag{4.8}$$

Where, Q_{conv1} and Q_{conv2} state convective heat fluxes from flow inside the shield and outside the shield respectively. Q_{rad1} and Q_{rad2} stand for radiative heat fluxes between shield-wall and shield- TC wire respectively.

$$Q_{conv1} = h_{c1} * A_{shield\ inner\ surface} * \left(T_{flow} - T_{shield}\right) \tag{4.9}$$

$$Q_{conv2} = h_{c2} * A_{shield\ outer\ surface} * \left(T_{flow} - T_{shield}\right) \tag{4.10}$$

For the Q_{conv1}, h_c is calculated as described in Section 4.1. As for Q_{conv2} flat plate correlation is used as the flow resembles an external flow around the flat plate.

$$Nu = 0.038 * Re_l^{0.8} * Pr^{1/3} \tag{4.11}$$

As inspected in section 2.6.1 flow on the external surface of the shield separates due to the sharp corner of the shield inlet and flow deflects in this region. Flow velocity isn't as high as the freestream value. After a visual inspection, flow velocities are thought to be 0.1 M in this region to be conservative on the HTC value because determining a greater value leads to higher HTC and lower radiation error.

$$Q_{rad1} = \sigma * \varepsilon * A_{shield\ outer\ surface} * \left({T_{shield}}^4 - {T_w}^4\right) \tag{4.12}$$

$$Q_{rad2} = \sigma * \varepsilon * A_{shield\ inner\ surface} * \left({T_{junction}}^4 - {T_{shield}}^4\right) \tag{4.13}$$

Where T_w is surrounding wall surface temperature, σ is Boltzmann constant, ε is the emissivity of the thermocouple junction.

For TC wire temperature,

$$Q_{conv} + Q_{rad} = 0 \tag{4.14}$$

$$Q_{conv} = h_c * A_{TC\ Wires\ Outer\ Surface} * \left(T_{flow} - T_{wire}\right) \tag{4.15}$$

Q_{rad} will be equal to equation 4.12. An iterative scheme is used as any of the shield and junction temperatures aren't known as apriori. For a specific shield temperature, the junction temperature is calculated and then heat fluxes are checked whether they are providing the equations above.

In Figures 4.9 and 4.10, radiation error distributions are presented for Duct Wall Temperature (T_w) values of 500 K and 700 K respectively. Calculations were made on the case of 5 bar and 1000 K as in Section 4.2. Application of the shield is observed to be a very effective precaution as the errors are less than %1.5 even in the very low-speed application of AR-4. As observed in Table 4.2, the AR-4 case results deviate for varying Mach numbers. This can be explained by the fact that the flow deceleration reaches very low levels and the effect on HTC is much greater than the other cases. AR-1 and 2 cases are observed to be less dependent on the Mach number. Although error percentages are low, for AR-4 radiation error reached 10 K for 1000 K flow total temperature. To decrease this error AR value may be increased. Thus, experimentalists must keep in mind applying a higher AR if the flow velocities are low in the measurement location.

Table 4.2: Radiation Error Values for Varying *Tw.*

Radiation Error Values (0.6 M, 5 bar, 1000 K inlet)			
	1	2	4
T_w- 500 K (0.6 M)	996.43	990.97	986.34
T_w- 500 K (0.3 M)	996.6	991.33	987.6
T_w- 700 K (0.6 M)	997.2	993.13	989.18
T_w- 700 K (0.3 M)	997.3	993.4	989.82

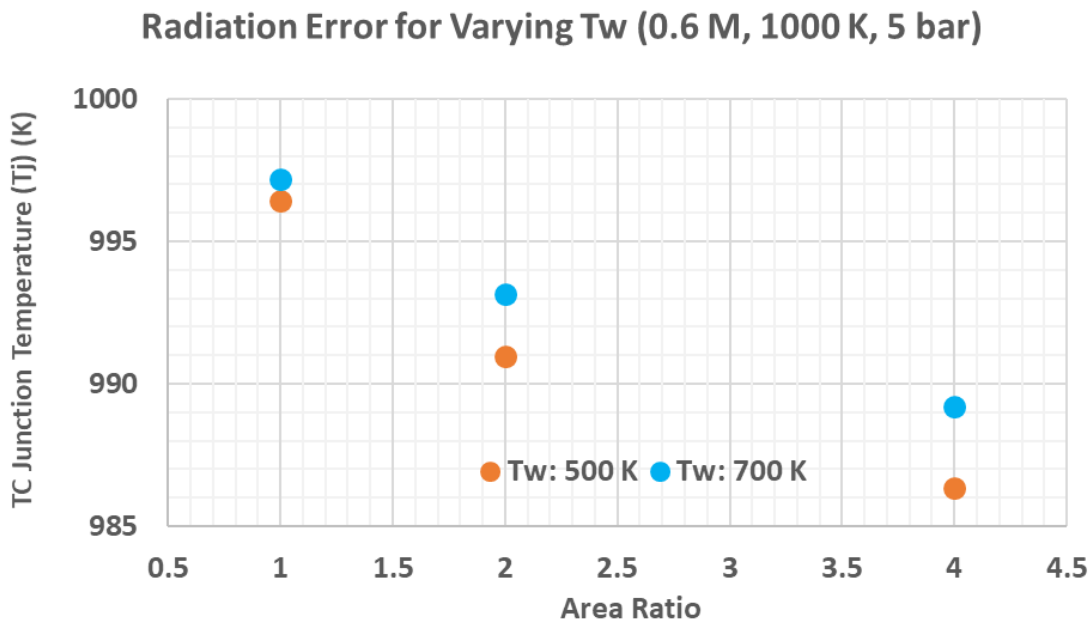

Figure 4.7: Radiation Error Distribution for Varying *Tw* at 0.6 M Case.

5. CONCLUSION

Flow structures inside and around a total temperature probe were investigated by applying CHT simulations on a case from the literature. CHT simulation results are in harmony with the experimental data regarding TC junction temperature so they are thought to be showing flow structures accurately.

The main aim of the total temperature probe design is to decrease flow velocities inside of the shield to avoid thermal conduction in the boundary layer around the TC junction. Simulation results showed that this aim is accomplished using a bleed hole strategy in which smaller area bleed holes control the mass flow rate entering the shield. Even for the 0.9 M case, flow velocity inside the shield decreases down to 0.25 M. For moderate flow angles, no flow separation occurs at the inlet of the shield and flow has a streamlined nature. On the outer surface of the probe shield, a large separation region occurred as expected due to the sharp corner. Flow reattached before reaching bleed holes and this separation region didn't cause any further limitation on the mass flow rate inside of the shield.

A parametric study was carried out in which the effects of flow angle, shield-to-bleed holes area ratio, temperature and pressure were investigated. Up to 20 degrees, flow angle effects are observed to be negligible. AR greater than 2 is unnecessary because the recovery factor didn't improve. The effect of temperature was observed to be dependent on the Prandtl number of specific conditions. The effect of pressure was observed to be dependent on the Reynolds number of the flow.

Convective heat transfer between flow and TC junction was modelled using outputs of CHT simulations. Errors due to conduction and radiation were modelled using basic heat transfer theory. Although the precautions to avoid these error mechanisms are effective, they may deviate TC junction temperature at considerable values. TC wire length and AR are parameters that may be used to avoid these errors. But experimentalists must carefully examine other features of the flow field before such applications.

REFERENCES

[1] Cengel, Y. A., Boles, M. A., & Kanoğlu, M. (2011). *Thermodynamics: an engineering approach* (Vol. 5, p. 445). New York: McGraw-hill.

[2] "Thermocouples Operating Principles," *www.msm.cam.ac.uk*. https://www.msm.cam.ac.uk/utc/thermocouple/pages/ThermocouplesOperatingPrinciples.html [Accessed: 12.03.2023].

[3] Saravanamuttoo, H. I. (1990). Recommended Practices for Measurement of Gas Path Pressures and Temperatures for Performance Assessment of Aircraft Turbine Engines and Components (Les Methodes Recommandees pour la Mesure de la Pression et de la Temperature de la Veine Gazeuse en Vue de l'Evaluation des Performances des Turbines Aeronautiques et de leurs Composants. *ADVISORY GROUP FOR AEROSPACE RESEARCH AND DEVELOPMENT NEUILLY-SUR-SEINE (FRANCE)*.

[4] Vincent, T. G., Rolfe, E. N., Lowe, K. T., & Schetz, J. A. (2019). Aerodynamic analysis of total temperature probe thermal performance using conjugate heat transfer. *Journal of Thermophysics and Heat Transfer*, *33*(3), 830-843.

[5] Paniagua, G., De´ nos, R., & Oropesa, M. (2002). *Thermocouple probes for accurate temperature measurements in short-duration facilities* (Vol. 3607, pp. 209-217).

[6] Wood, R. D. (1959). An Experimental Investigation of Hypersonic Stagnation Temperature Problems.

[7] King, W. J. (1943). Measurement of high temperatures in high-velocity gas streams. *Transactions of the American Society of Mechanical Engineers*, *65*(5), 421-428.

[8] Goldstein, D. L., & Scherrer, R. (1949). *Design and calibration of a total-temperature probe for use at supersonic speeds* (No. NACA-TN-1885).

[9] Scadron, M. D., & Warshasky, I. (1952). *Experimental determination of time constants and Nusselt numbers for bare-wire thermocouples in high-velocity air streams and analytic approximation of conduction and radiation errors* (No. NACA-TN-2599).

[10] Stickney, T. M. (1955). *Recovery and time-response characteristics of six thermocouple probes in subsonic and supersonic flow* (No. NACA-TN-3455).

[11] Dahl, A. I., & Fiock, E. F. (1950). Response characteristics of temperature sensing elements for use in the control of jet engines. *J. Research Natl. Bur. Standards*, *45*(4).

[12] Glawe, G. E., Holanda, R., & Krause, L. N. (1978). *Recovery and radiation corrections and time constants of several sizes of shielded and unshielded thermocouple probes for measuring gas temperature* (No. NASA-TP-1099).

[13] Moffat, R. J. (1962). Gas temperature measurement. *Temperature; Its Measurement and Control in Science and Industry, Volume 2*, 553.

[14] Villafañe, L., & Paniagua, G. (2013). Aero-thermal analysis of shielded fine wire thermocouple probes. *International Journal of Thermal Sciences*, *65*, 214-223.

[15] Schneider, A. J. (2015). *Computational modeling of total temperature probes* (Doctoral dissertation, Virginia Tech).

[16] Zou, Z., Yang, W., Zhang, W., Wang, X., & Zhao, J. (2018). Numerical modeling of steady state errors for shielded thermocouples based on conjugate heat transfer analysis. *International Journal of Heat and Mass Transfer*, *119*, 624-639.

[17] Glawe, G. E., Simmons, F. S., & Stickney, T. M. (1956). *Radiation and recovery corrections and time constants of several chromel-alumel thermocouple probes in high-temperature, high-velocity gas streams* (No. NACA-TN-3766).

[18] Ansys, Inc. (2020). ANSYS Fluent-Theory Guide-Release 2020R1.

[19] Menter, F. R. (1994). Two-equation eddy-viscosity turbulence models for engineering applications. *AIAA journal*, *32*(8), 1598-1605.

[20] Touloukian, Y. S., Powell, R. W., Ho, C. Y., & Klemens, P. G. (1971). *Thermophysical properties of matter-the tprc data series. volume 2. thermal conductivity-nonmetallic solids.(reannouncement). data book* (No. AD-A-951936/4/XAB). Purdue Univ., Lafayette, IN (United States). Thermophysical and Electronic Properties Information Center.

[21] Touloukian, Y. S., & Buyco, E. H. (1971). *Thermophysical properties of matter-the TPRC data series. Volume 4. Specific heat-metallic elements and alloys*. Thermophysical and Electronic Properties Information Analysis Center Lafayette IN.

[22] Zografos, A. I., Martin, W. A., & Sunderland, J. E. (1987). Equations of properties as a function of temperature for seven fluids. *Computer Methods in Applied Mechanics and Engineering*, *61*(2), 177-187.

[23] Cengel, Y. A., Ghajar, A. J., & Kanoglu, M. (2011). Heat and mass transfer: fundamentals and applications. *(No Title)*.

CURRICULUM VITAE

PHOTO

Name Surname : Erdem Meriç

EDUCATION

- **B.Sc.** **:** 2019, Istanbul Technical University, Faculty of Aeronautics and Astronautics, Aeronautical Engineering
- **M.Sc.** **:** 2023, University, Istanbul Technical University, Faculty of Aeronautics and Astronautics, Aeronautical and Astronautical Engineering

PROFESSIONAL EXPERIENCE AND REWARDS:

- 2019 – 2020 Mechanical Design Engineer, TEI
- 2020 – 2020 Aerodynamics Engineer, TEI
- 2021 – Aerodynamic Test Engineer, Kale Ar-ge

PUBLICATIONS, PRESENTATIONS AND PATENTS ON THE THESIS:

- **Meriç, E., Edis F. E.** 2023: A Numerical Investigation of Total Temperature Probes Measurement Performance, RAST, June 03-06, 2023 Istanbul, Turkey.